Correlations in nondegenerate parametric oscillation. II. Below threshold results

P. D. Drummond
Physics Department, The University of Queensland, Saint Lucia, Queensland 4067, Australia

M. D. Reid
Physics Department, University of Waikato, Private Bag, Hamilton, New Zealand
(Received 24 July 1989)

We develop the quantum theory of a driven, damped intracavity parametric oscillator in the case of nondegenerate signal and idler modes. An analysis of the results of different types of local-oscillator measurements on the outgoing modes is presented. The frequency-domain squeezing is calculated below threshold including the effect of detunings and nonequal decay rates. We also calculate a *nonclassical* correlation in the quadrature amplitudes of the output beams. The existence of an Einstein-Podolsky-Rosen paradox is demonstrated through violations of the inferred Heisenberg uncertainty principle at causally unrelated locations in the output field. This provides a way of maintaining the commutation relations of the measured operators in the exact form envisaged originally by Einstein, Podolsky, and Rosen.

I. INTRODUCTION

Squeezing is the noise reduction that can occur in a quantum field when the quantum fluctuations in one of the field quadrature phases are reduced below the usual vacuum level.[1-4] In the case of the observed squeezing in electromagnetic traveling-wave fields, this feature is evidenced by the reduction of the noise in a photodetector below the shot-noise level.

As squeezing is phase sensitive, this is generally achieved by means of a local-oscillator experiment, where an intense local oscillator is mixed with the squeezed field prior to photodetection. The local-oscillator phase is then varied, and a cyclic variation in the apparent noise level is observed. Owing to technical noise that predominates at low frequencies, it is usual to Fourier analyze the spectrum. Squeezing is said to occur when the intensity correlation spectrum is reduced below the shot-noise level at any frequency, given an appropriate phase angle between the input and the local oscillator.

This type of noise reduction has numerous potential applications ranging from gravity-wave detection[4] to ultrasensitive interferometry.[5] Following the landmark experiments of Slusher *et al.*, squeezing has now been observed in several laboratories.[6] One of the more successful techniques to data is practiced by Wu *et al.*,[6] who use degenerate parametric oscillation or subharmonic generation in an interferometer.[7-12] However , it is also possible, and often simpler in practice, to operate a parametric oscillator in a nondegenerate mode of operation.[13-18] Heidmann *et al.*[16] have recently reported an experimental reduction of intensity difference fluctuations in the nondegenerate parametric oscillator. In this paper, we analyze the intracavity nondegenerate parametric oscillator below threshold and determine the extent of noise reduction in this situation. We include detunings, pump depletion, and damping. The above threshold results were presented in an earlier paper.[18] Related calculations for squeezing were recently presented by Collett and Loudon,[15] Reynaud *et al.*,[16] and Björk and Yamamoto.[17]

We also present a detailed analysis of the types of local-oscillator measurements that can be utilized in this twin-beam case. The usual single-beam measurements involve the intensity spectrum[19] and the local-oscillator (or "squeezing") spectrum.[20,21] In addition, there are now correlations between the two output beams. These can be observed as direct intensity correlation using two detectors,[16,22] as "two-mode" squeezing with one local oscillator and one detector,[23] or by measurements of twin local-oscillator quadrature correlations ("four-mode squeezing").[24] Experiments showing strong quadrature correlations were recently undertaken for nondegenerate four-wave mixing in an optical fiber.[25] We therefore wish to analyze the quadrature correlation experiments for the nondegenerate parametric oscillator. The single-local-oscillator and dual-local-oscillator measurements are discussed and a "squeezing spectrum" is defined in each case.

The application of nondegenerate correlation is most evident in the dual-detector experiments. Proposed applications include ultrasensitive spectroscopy[16] and quantum nondemolition measurement schemes.[25,26] In these applications, information about the signal is gained by performing measurements on the idler. There is a correlation between particular quadrature phase amplitudes of the signal and idler: the quantum noise of each is correlated. We calculate this correlation, first in terms of a Cauchy-Schwarz inequality, and secondly in terms of the variance of an appropriately normalized signal and idler quadrature amplitude difference. This last quantity, defined originally by Levenson and Shelby,[25] tells us the average error in inferring the signal amplitude for a given value of the idler amplitude. These correlation measurements are directly related to the dual-local-oscillator squeezing spectrum.

There has also been recent interest in the nondegen-

erate oscillator (or amplifier) from the viewpoint of providing tests of classical theores versus quantum theory.[27] These tests have been concerned with photon counting and intensity correlations between signal and idler. We point out that our study extends beyond intensity correlations to include correlations in phase. We discuss how sufficient correlation between signal and idler for two noncommuting quadrature amplitudes is an example of the original Einstein-Podolsky-Rosen[28] (EPR) paradox. This has been discussed in part in a previous publication.[29,30]

II. HAMILTONIAN AND STOCHASTIC EQUATIONS

We shall use a standard procedure for analyzing the optical parametric oscillator. The nonlinear medium is treated as providing a nonlinear term in the Hamiltonian of the electromagnetic field in the interferometer, provided that the nonlinear absorption is small. This technique is successful in predicting the results of other parametric oscillator experiments. Accordingly, it clearly is a good approximation for the analysis of this type of nonlinear medium. After quantizing the Hamiltonian,[9,13] the nonlinear medium can be shown to generate cubic terms in the mode operators in the rotating-wave approximation.

All the modes of the problem are fully quantized, but only the relevant, near-resonant, intracavity modes need to be included. A reservoir of extracavity modes is necessary to allow for the damping of the oscillator modes to the environment and to the detectors. An intense, coherent input driving field is included at a pump frequency defined as $2\omega_0$. Hence, in the rotating-wave approximation, the Hamiltonian is given by[13,14]

$$\hat{H}=\hat{H}_{\rm rev}+\hat{H}_{\rm irrev} , \tag{2.1}$$

where

$$\begin{aligned}\hat{H}_{\rm rev}&=\hbar\omega_1\hat{a}_1^{\dagger}\hat{a}_1+\hbar\omega_2\hat{a}_2^{\dagger}\hat{a}_2+\hbar\omega_3\hat{a}_3^{\dagger}\hat{a}_3\\&\quad+i\hbar g(\hat{a}_1^{\dagger}\hat{a}_2^{\dagger}\hat{a}_3-\hat{a}_1\hat{a}_2\hat{a}_3^{\dagger})\\&\quad+i\hbar[E\hat{a}_3^{\dagger}\exp(-2i\omega_0 t)-E^*\hat{a}_3\exp(2i\omega_0 t)] ,\\\hat{H}_{\rm irrev}&=\hat{a}_1\hat{\Gamma}_1^{\dagger}+\hat{a}_1^{\dagger}\hat{\Gamma}_1+\hat{a}_2\hat{\Gamma}_2^{\dagger}+\hat{a}_2^{\dagger}\hat{\Gamma}_2+\hat{a}_3\hat{\Gamma}_3^{\dagger}+\hat{a}_3^{\dagger}\hat{\Gamma}_3 .\end{aligned}$$

Here ω_1, ω_2, and ω_3 are the signal, idler, and pump mode frequencies, respectively. The term g describes the nonlinear coupling term due to the medium, and E is proportional to the input amplitude at frequency $2\omega_0$. We assume that the modes have the wave-vector-matching condition of $\omega_3\approx\omega_2+\omega_1$. The input frequency $2\omega_0$ can, however, be off resonant with ω_3, so in principle all of these four frequencies could be independent. The operators $\hat{a}_i$ and $\hat{a}_i^{\dagger}$ are the boson annihilation and creation operations for the signal, idler, and pump modes. With no loss of generality, the quantum phases of the states can always be chosen so that g is real and positive. We assume that other cavity modes do not couple strongly to the modes of interest.

The decay of the cavity to the external modes of the electromagnetic field is described by the reservoir operators, $\hat{\Gamma}_i$ and $\hat{\Gamma}_i^{\dagger}$, which are sums over the external field operators in a standard notation. These will give rise to cavity damping rates κ_1^0, κ_2^0, κ_3^0, respectively, which are assumed to be small compared to the resonant frequencies and the intracavity mode spacings. In the special case of $\omega_1=\omega_2$, it is necessary that the signal and idler modes have orthogonal polarizations, since we assume that all modes decay to distinct, uncorrelated reservoirs. As is usual, the equations of motion for the density matrix can be readily transformed to a master equation on tracing over the external reservoirs. This is most readily accomplished in an interaction picture relative to the input frequency ω_0, and two frequencies, ω_1^0 and ω_2^0, for the signal and idler modes, respectively. These are defined so that the free Hamiltonian $\hat{H}_0$, which determines the interaction picture operator evolution, is

$$\hat{H}_0=\hbar\sum_j\omega_j^0\hat{a}_j^{\dagger}\hat{a}_j ,$$

where

$$\begin{aligned}&\omega_1^0=\omega_0+\epsilon\approx\omega_1 ,\\&\omega_2^0=\omega_0-\epsilon\approx\omega_2 ,\\&\omega_1^0+\omega_2^0=\omega_3^0=2\omega_0\approx\omega_3 .\end{aligned} \tag{2.2}$$

The frequencies $\omega_j^0=\omega_0\pm\epsilon$ are the characteristic oscillations frequencies of the signal and idler modes when driven externally by the pump at $2\omega_0$. Here ω_0 is the central frequency which can be used as a local-oscillator frequency during detection of squeezing. The frequency offset ϵ will be chosen later. We note that any detunings of the cavity modes,

$$\Delta_n=(\omega_n-\omega_n^0) , \tag{2.3}$$

must then be relatively small compared to the mode spacings in order for the single-mode description to be valid. The resulting master equation[31] in the Markovian approximation for the reduced density operator $\hat{\rho}$ in the interaction picture is

$$\begin{aligned}\partial_t\hat{\rho}&=(i\hbar)^{-1}[\hat{H}_{\rm rev}^{I},\hat{\rho}]\\&\quad+\sum_j\kappa_j^0(2\hat{a}_j\hat{\rho}\hat{a}_j^{\dagger}-\hat{a}_j^{\dagger}\hat{a}_j\hat{\rho}-\hat{\rho}\hat{a}_j^{\dagger}\hat{a}_j)\\&\quad+2\sum_j\kappa_j^0 n_j^{\rm th}[[\hat{a}_j,\hat{\rho}],\hat{a}_j^{\dagger}] ,\end{aligned} \tag{2.4}$$

where

$$\partial_t\equiv\frac{\partial}{\partial t} .$$

Here κ_j^0 are the damping constants (amplitude decay rates) of the modes, and $n_j^{\rm th}$ are the thermal photon occupation numbers of the external reservoirs. These can also approximately describe any wideband background radiation due to nonthermal sources. The term $\hat{H}_{\rm rev}^{I}$ is the reversible part of the interaction picture Hamiltonian. Owing to the frequency matching with ω_0 used to define the interaction picture, this is given by

$$\begin{aligned}H_{\rm rev}^{I}&=\sum_j\hbar\Delta_j\hat{a}_j^{\dagger}\hat{a}_j+i\hbar g(\hat{a}_1^{\dagger}\hat{a}_2^{\dagger}\hat{a}_3-\hat{a}_1\hat{a}_2\hat{a}_3^{\dagger})\\&\quad+i\hbar(E\hat{a}_3^{\dagger}-E^*\hat{a}_3) .\end{aligned} \tag{2.5}$$

We note that all operators $\hat{a}_j, \hat{a}_j^\dagger$, without time arguments, are in the Schrödinger picture and do not evolve in time. Thus the interaction picture operators have a time evolution given by

$$\hat{a}_j^I(t)=\hat{a}_j \exp(-i\omega_j^0 t) ,$$
$$[\hat{a}_j^I(t)]^\dagger=\hat{a}_j^\dagger \exp(i\omega_j^0 t) . \tag{2.6}$$

Owing to the choice of interaction picture defined relative to the input frequency ω_0, there is no explicit time dependence in the reversible part of the interaction picture Hamiltonian, which greatly simplifies the solution of the master equation. For later use, a complex decay and detuning parameter κ_1 is defined for each mode:

$$\kappa_j \equiv \kappa_j^0 + i\Delta \equiv \kappa_j^0 e^{-i\theta_j} . \tag{2.7}$$

As the choice of ω_1^0, ω_2^0 is arbitrary, it is always possible to choose the detunings to be equal relative to the decay time, so that $\kappa_1 \kappa_2^*$ can always be chosen to be real. This is obtained by choosing ϵ so that

$$\epsilon = \frac{(\omega_1-\omega_0)\kappa_2^0 - (\omega_2-\omega_0)\kappa_1^0}{\kappa_2^0+\kappa_1^0} . \tag{2.8}$$

We shall prove in the following sections that this is in fact the optimal choice of interaction picture, in the sense that it leads to semiclassical behavior that is time invariant above the oscillation theshold.

A systematic treatment of the master equation (2.4) is most simply obtained in an operator representation of $\hat{\rho}$. In this representation, $\hat{\rho}$ is expanded in a basis of coherent state[19] projection operators. Here a coherent state is denoted $|\alpha_1,\alpha_2,\alpha_3\rangle$ for modes 1, 2, and 3, respectively. The expansion coefficient or P function is not unique. However, it is always possible to choose it as a positive function $P(\boldsymbol{\alpha})$,[32] so that

$$\hat{\rho} = \int [|\boldsymbol{\alpha}\rangle\langle\boldsymbol{\alpha}^\dagger| / (\langle\boldsymbol{\alpha}^\dagger|\boldsymbol{\alpha}\rangle)] P(\boldsymbol{\alpha},\boldsymbol{\alpha}^\dagger) d^6\boldsymbol{\alpha}\, d^6\boldsymbol{\alpha}^\dagger ,$$

where

$$\boldsymbol{\alpha} \equiv (\alpha_1,\alpha_2,\alpha_3) ,$$
$$\boldsymbol{\alpha}^\dagger \equiv (\alpha_1^\dagger,\alpha_2^\dagger,\alpha_3^\dagger) . \tag{2.9}$$

With this representation, it is easily shown that $P(\boldsymbol{\alpha},\boldsymbol{\alpha}^\dagger)$ must satisfy a Fokker-Planck equation for its time development which has only second-order derivative terms in $(\boldsymbol{\alpha},\boldsymbol{\alpha}^\dagger)$. In the limit of $n_j^{\rm th} \to 0$, which is appropriate for optical laser experiments, the Fokker-Planck equation can be directly obtained to be[14]

$$\begin{aligned}\partial_t P(\boldsymbol{\alpha},\boldsymbol{\alpha}^\dagger) = [&\partial_1(\kappa_1\alpha_1 - g\alpha_2^\dagger\alpha_3) + \partial_2(\kappa_2\alpha_2 - g\alpha_1^\dagger\alpha_3) \\ &+ \partial_3(\kappa_3\alpha_3 - E + g\alpha_1\alpha_2) \\ &+ \partial_{12}^2(g\alpha_3) + \text{H.c.}]P(\boldsymbol{\alpha},\boldsymbol{\alpha}^\dagger) ,\end{aligned} \tag{2.10}$$

where

$$\partial_i \equiv \frac{\partial}{\partial\alpha_i} .$$

Here H.c. indicates terms obtained by interchanging κ_i with κ_i^* and α_i with $\alpha_i^\dagger$. In this equation only analytic derivatives of $\boldsymbol{\alpha},\boldsymbol{\alpha}^\dagger$ appear. While this equation has a nonpositive-definite diffusion coefficient, there is an equivalent form with a positive-definite diffusion. This corresponds to six stochastic differential equations in the variables $(\boldsymbol{\alpha},\boldsymbol{\alpha}^\dagger)$:

$$\begin{aligned}\partial_t\alpha_1 &= -\kappa_1\alpha_1 + g\alpha_3\alpha_2^\dagger + (g\alpha_3)^{1/2}\xi_1(t) ,\\ \partial_t\alpha_2 &= -\kappa_2\alpha_2 + g\alpha_3\alpha_1^\dagger + (g\alpha_3)^{1/2}\xi_2(t) ,\\ \partial_t\alpha_3 &= E - \kappa_3\alpha_3 - g\alpha_1\alpha_2 ,\\ \partial_t\alpha_1^\dagger &= -\kappa_1^*\alpha_1^\dagger + g\alpha_3^\dagger\alpha_2 + (g\alpha_3^\dagger)^{1/2}\xi_1^\dagger(t) ,\\ \partial_t\alpha_2^\dagger &= -\kappa_2^*\alpha_2^\dagger + g\alpha_3^\dagger\alpha_1 + (g\alpha_3^\dagger)^{1/2}\xi_2^\dagger(t) ,\\ \partial_t\alpha_3^\dagger &= E^* - \kappa_3^*\alpha_3^\dagger - g\alpha_1^\dagger\alpha_2^\dagger ,\end{aligned} \tag{2.11}$$

where

$$\langle\xi_1(t)\xi_2(t')\rangle = \delta(t-t') ,$$
$$\langle\xi_1^\dagger(t)\xi_2^\dagger(t')\rangle = \delta(t-t') .$$

All other correlation functions of the noise vanish, except those specified. It should be noted that the correlations of the fluctuating quantities $\boldsymbol{\alpha}$ and $\boldsymbol{\alpha}^\dagger$ correspond directly to normally ordered, time-ordered correlation functions of operators. Since these are the quantities directly measured in photon correlation experiments, the stochastic equations generate directly the observed moments. However, this correspondence is only true for ensemble-averaged correlation functions. The continuous stochastic trajectories should not be regarded as having a one-to-one correspondence with experimental observations of discrete photon counts, since these are not continuous events.

The choice of a normally ordered representation as utilized here results in an extremely simple nonlinear set of equations. These enable us to directly calculate time-ordered, normally ordered correlations or moments of the intracavity operators. It is easily shown that ordered correlations of Heisenberg picture operators $\hat{a}_i(t)$ are given by

$$\begin{aligned}\langle :\hat{a}_i(t)\hat{a}_j(t'):\rangle &= \langle\alpha_i(t)\alpha_j(t')\rangle e^{-i\omega_i^0 t - i\omega_j^0 t} ,\\ \langle\hat{a}_i^\dagger(t)\hat{a}_j(t')\rangle &= \langle\alpha_i^\dagger(t)\alpha_j(t')\rangle e^{i\omega_i^0 t - i\omega_j^0 t} .\end{aligned} \tag{2.12}$$

Thus there is a direct correspondence between time-ordered, normally ordered operator moments and stochastic moments. This correspondence also extends to time-ordered, normally ordered products with larger numbers of arguments which occur (for example) in intensity correlation functions. We denote these products with ordering symbols: (: :). Here annihilation operators are ordered with earlier times to the right and creation operators with earlier times to the left. In Sec. III we relate these internal operator correlations to a set of internal intensity and correlation spectra, denoted $s(\omega)$ and $c(\omega)$. These in turn are used to obtain the observed correlations and spectra in external measurements. We use the notation $G^{(n)}(t_1,\ldots,t_n)$ as usual for external photon-counting correlations. We also use the notation $V(\omega)$ to denote an observed normalized spectral variance

in the heterodyne detected current. $S(\omega)$ is used to denote the squeezing spectrum, or departure from classical statistics. Finally, we introduce $\Delta^2(\omega)$ to indicate an inference spectrum in an EPR-type experiment.

III. CORRELATIONS AND SQUEEZING: TYPES OF MEASUREMENT

Before proceeding to solve Eqs. (2.11), we first analyze the results of measurements on the fields produced by the parametric amplifier. In practice, measurements of the external fields of a cavity are simpler to achieve than the intracavity measurements that our stochastic variables describe most directly. This relationship is discussed by Yurke[11] and by Collett and Gardiner,[12] who have demonstrated how the output fields of a cavity can be described precisely in terms of the internal fields. The measurements of most interest here are those obtained with local oscillators. There can be either one or two local oscillators in nondegenerate parametric amplifier experiments, as the output field can be split up into its independent components prior to detection. This is shown in Figs. 1 and 2. The simplest case is that of the single local oscillator, with two identically polarized output beams. The case of orthogonally polarized output beams will be regarded as a twin-local-oscillator experiment, because here the local oscillator must be treated as having two orthogonal components also. The single- and twin-local-oscillator cases will be treated individually.

A. Single-local-oscillator case

In this case we divide up the input fields of the cavity into orthogonal modes denoted $\hat{a}_k$. These are transversely phase matched to the internal modes with which they are nearly resonant. We define these Heisenberg picture input and output fields $\hat{\Phi}_i^{\text{in}}$ and $\hat{\Phi}_i^{\text{out}}$ so that $\langle[\hat{\Phi}_i^{\text{out}}(t,x)]^\dagger\hat{\Phi}_i^{\text{out}}(t,x)\rangle$ for $x>0$ is the photon flux out of the ith mode integrated over the mode cross section. We note that in a one-dimensional treatment of the external field, $\hat{\Phi}_i^{\text{in}}$ and $\hat{\Phi}_i^{\text{out}}$ can be readily expanded in the external-field mode operators $\hat{a}_k$ quantized over a length

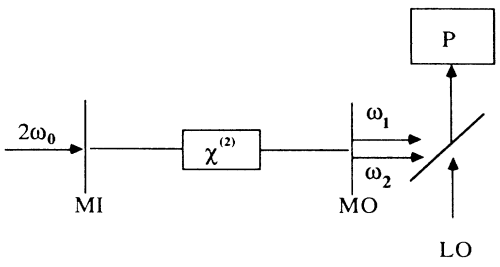

FIG. 1. Typical experiment for correlations in nondegenerate parametric oscillation. An input pump at $2\omega_0$ produces outputs at ω_1,ω_2. The input mirror, MI, is highly reflective at the signal and idler frequencies. The output mirror MO is relatively more transmissive. The beam splitter is highly reflecting, or could be replaced by dual-homodyne detectors. The local oscillator at ω_0 combines with the signal and idler to produce an interference signal at the photodiode, in the simplest case.

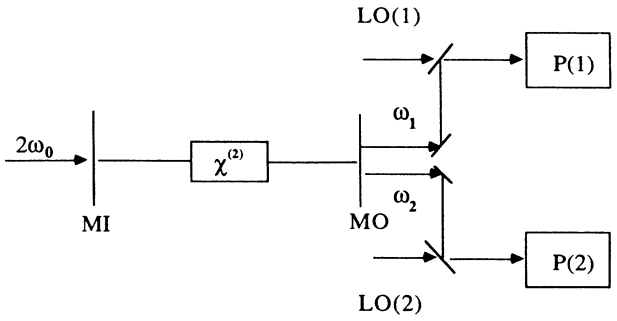

FIG. 2. In the twin-detector case, a similar output is produced to that in Fig. 1, but is incident on two detectors using two local oscillators.

L (where we shall take the limit of $L\to\infty$):

$$\hat{\Phi}_i^{\text{out}}(t,x)=\left[\frac{c}{L}\right]^{1/2}\sum_{k=k_i^0-\Delta k}^{k_i^0+\Delta k}\hat{a}_k(t)e^{ikx}\ ,$$
$$\hat{\Phi}_i^{\text{in}}(t,x)=\left[\frac{c}{L}\right]^{1/2}\sum_{k=-k_i^0-\Delta k}^{-k_i^0+\Delta k}\hat{a}_k(t)e^{ik}\ , \tag{3.1}$$

where

$$ck_i^0=\omega_i^0\ .$$

It is clear from this that $\hat{\Phi}_i$ is restricted to a range of wave numbers near the ith mode resonance.

In the three-dimensional case, we use the paraxial approximation to treat propagation. The forward-propagating electric field $\hat{\mathbf{E}}$ at location $\mathbf{x}$ in the external field is given by extending the ith internal mode function into a phase-matched external transverse mode $\mathbf{u}_i$, for $x>0$:

$$\hat{E}^{\text{out}}(t,\mathbf{x})=\sum_i\left[\frac{\hbar\omega_i}{2\epsilon_0 c}\right]^{1/2}\mathbf{u}_i(\mathbf{x})\hat{\Phi}_i^{\text{out}}(t,x)\ , \tag{3.2}$$

where

$$\int|\mathbf{u}_i(\mathbf{x})|^2d^2\mathbf{r}=1,\quad \mathbf{x}=(x,\mathbf{r})\ .$$

Thus, $\hat{\Phi}_i^{\text{out}}$ can be directly related to the internal operator for the mode with internal mode function $\mathbf{u}_i$, through boundary conditions on the electric field $\mathbf{E}$ at the cavity output mirror. These imply that

$$\hat{a}_i(t)=(2\kappa_i^1)^{-1/2}[\hat{\Phi}_i^{\text{in}}(t,x=0)+\hat{\Phi}_i^{\text{out}}(t,x=0)]\ , \tag{3.3}$$

where

$$\kappa_i^0\geq\kappa_i^1\ .$$

Here $(\kappa_i^1)^{-1/2}$ is proportional to the output coupler transmissivity, while κ_i^0 describes all the lumped losses including those due to losses through other mirrors, as well as absorption and scattering in the intracavity medium. In the absence of these losses, $\kappa_i^0=\kappa_i^1$, which gives the optimal squeezing in the external field.

In the case of a squeezing measurement, a coherent local oscillator is present at the detector in addition to the output fields. Measurements of this type were originally discussed using a non-normally ordered theory of the measurement process.[20] However, it is more useful, especially when calculating the shot-noise component, to use the more standard normally ordered photodetection theory.[19] This has been recently used to treat single-local-oscillator measurements.[21] For completeness, we now summarize the single-local-oscillator results in our notation. Our results give the observed current spectra in terms of the relevant intracavity mode correlation spectra, which will be calculated in the following sections.

As the squeezing occurs in a quadrature which combines the signal and idler fields, it is necessary that these fields should be combined at the detector. The detector is then illuminated with an intense local oscillator with coherent amplitude $\Phi_0=\langle\hat{\Phi}_0\rangle$ at the central frequency ω_0. The overall one-time and two-time correlation functions for photodetection with perfect mode matching at the detector location $x=x_d$ are given by time-ordered, normally ordered correlation functions:[19]

$$G^{(1)}(t)=I(t)=\langle\hat{I}(t)\rangle$$

and (3.4)

$$G^{(2)}(t,t')=\langle:\hat{I}(t)\hat{I}(t'):\rangle\ .$$

Here, we define $\hat{I}(t)$ as the local photon flux operator at the detector, in the Heisenberg picture:

$$\hat{I}(t)=\left[\nu_0^*\hat{\Phi}_0^\dagger e^{i\omega_0 t}+\sum_j \nu_j^*\hat{\Phi}_j^\dagger(t)\right]\times\left[\nu_0\hat{\Phi}_0 e^{-i\omega_0 t}+\sum_j \nu_j\hat{\Phi}_j(t)\right], \tag{3.5}$$

where

$$\hat{\Phi}_j(t)\equiv\hat{\Phi}_j^{\rm out}(t,x_d)\ .$$

The complex factors ν_0,ν_1,ν_2 allow for the detector efficiency and the amplitude of combining the local oscillator with the signal fields, so that

$$|\nu_0|^2+|\nu_j|^2\le 1,\quad j=1,2\ . \tag{3.6}$$

For simplicity, we suppose that a beam splitter is used with $|\nu_0|\ll 1$ and ν_j is near $|\nu_j|=1$. This results in optimal squeezing, while predicting similar behavior to more complicated balanced homodyne schemes. The symbols (::) indicate that the two-time correlation function is time ordered and normally ordered. This implies that no contributions occur from the other modes in the vacuum state, which in any case could not be phase matched to the local oscillator over the entire detector area.

The phase angle between the local oscillator and the output field is defined by

$$i\theta_j=\ln\left[\frac{\nu_j|\nu_0\Phi_0|}{|\nu_j|\nu_0\Phi_0}\right]\ . \tag{3.7}$$

As we will find that the local-oscillator measurements only depend on the total phase $\theta_1+\theta_2$, it is useful to define an overall phase, $\theta=(\theta_1+\theta_2)/2$.

The quantity most often measured in experiment is the output current correlation function. We suppose each current pulse is $i_0(t-t_p)$ for a photon arriving at t_p. The total output current for photons arriving at times t_j is $i(t)$, with a current correlation function of G^I, where

$$\begin{aligned} i(t)&=\sum_j i_0(t-t_j)\ ,\\ G^I(t,t')&=\left\langle\sum_j i_0(t-t_j)i_0(t'-t_j)\right\rangle\\ &\quad+\left\langle\sum_j\sum_{\substack{k\\ j\neq k}} i_0(t-t_j)i_0(t'-t_k)\right\rangle\ . \end{aligned} \tag{3.8}$$

This has contributions both from the one-time correlation function (when $j=k$) and from the two-time correlation function (when $j\neq k$). We note that $G^{(2)}(t,t')$ is defined as the probability density of observing two photons, one at t and one at t'. Hence, combining these,

$$G^I(t,t')=\int I(t_1)[i_0(t-t_1)i_0(t'-t_1)]dt_1+\int\int G^{(2)}(t_1,t_2)[i_0(t-t_1)i_0(t'-t_2)]dt_1dt_2\ . \tag{3.9}$$

This expression is generally true for arbitrary current pulse shapes. For simplicity, we will suppose that $i_0(t)=Ze\delta(t)$. This implies the current pulses are short compared to the time scales (ω^{-1}) of interest and produce Z electrons in total. The first term is often called a shot-noise term, and is related to Poissonian number fluctuations. The observed low-frequency steady-state current correlation spectrum is therefore

$$G^I(\omega)=(Ze)^2\left[\langle\hat{I}(0)\rangle+\int e^{i\omega\tau}\langle:\hat{I}(0)\hat{I}(\tau):\rangle\,d\tau\right], \tag{3.10}$$

where we have defined

$$G^I(\omega)=\frac{1}{T}\int\int e^{i\omega(t'-t)}G^I(t,t')dt'dt\ . \tag{3.11}$$

Expanding and keeping terms to order $I^0=\langle|\nu_0|^2\hat{\Phi}_0^\dagger\hat{\Phi}_0\rangle$, we find that for a local oscillator uncorrelated with the signal,

$$\begin{aligned} G^I(\omega)=(Ze)^2I^0\Big[&1+2\pi\delta(\omega)(I^0+2I^s)+\int e^{i\omega\tau}\langle[\hat{\Phi}_s^\dagger(\tau)\hat{\Phi}_s(0)+\hat{\Phi}_s^\dagger(0)\hat{\Phi}_s(\tau)]\rangle d\tau\\ &+\int e^{i\omega\tau}\langle:[e^{i\omega_0\tau}\hat{\Phi}_s(0)\hat{\Phi}_s(\tau)+\text{H.c.}]:\rangle d\tau\Big], \end{aligned} \tag{3.12}$$

where

$$I^s \equiv \langle \hat{\Phi}_s^\dagger(0)\hat{\Phi}_s(0)\rangle \equiv \langle \hat{\Phi}_s^\dagger(t)\hat{\Phi}_s(t)\rangle \ .$$

Here we have defined $\langle \hat{\Phi}_s^\dagger(t)\hat{\Phi}_s(t)\rangle$ to correspond to the total *detected* signal photon flux, so that

$$\hat{\Phi}_s(t) \equiv \sum_j |\nu_j| e^{i\theta_j}\hat{\Phi}_j(t) \ . \tag{3.13}$$

Since the signal and idler can interfere coherently, it is useful to define a total quadrature field that includes both modes together with the relevant efficiency factors, i.e.,

$$\hat{X}^\theta(t) = \sum_j |\nu_j| e^{i\theta_j + i\omega_0 t}\hat{\Phi}_j(t) + \text{H.c.} \tag{3.14}$$

Thus $G^I(\omega)$ can be reexpressed in terms of the quadrature operators $\hat{X}^\theta(t)$. Normalizing by the shot-noise background, which equals $(Ze)^2 I^0$,

$$\frac{G^I(\omega)}{(Ze)^2 I^0} = 2\pi\delta(\omega)(I^0 + 2I^s) + 1 + \int \langle :\hat{X}^\theta(0)\hat{X}^\theta(\tau):\rangle e^{i\omega\tau} d\tau \ . \tag{3.15}$$

The last two terms comprise the shot-noise plus a term due to coherent interference between the local oscillator and the signal. This combination is called the squeezing variance $V(\theta,\omega)$, which is defined for an integration time T as

$$V(\theta,\omega) = 1 + 2\pi\langle :[\hat{X}^\theta(\omega)]^\dagger \hat{X}^\theta(\omega):\rangle / T \ , \tag{3.16a}$$

where

$$\hat{X}^\theta(\omega) \equiv \frac{1}{\sqrt{2\pi}} \int_{-T/2}^{T/2} e^{i\omega\tau}\hat{X}^\theta(t) dt \ .$$

Using the free-field commutation relations of the $\hat{\Phi}_s(t)$ field in the case $|\nu_j| = 1$, $V(\theta,\omega)$ can be rewritten as

$$V(\theta,\omega) = 2\pi\langle [\hat{X}^\theta(\omega)]^\dagger \hat{X}^\theta(\omega)\rangle / T, \quad |\nu_j| = 1 \ . \tag{3.16b}$$

We see that $V(\theta,\omega)$ is an expectation value of a positive-definite operator, with a lower bound of zero, and a value of unity for a normal vacuum or coherent input, in the case of perfect efficiency ($|\nu_j| = 1$). Here we use the fact that for perfect efficiency $[\hat{\Phi}_s(\omega), \hat{\Phi}_s^\dagger(\omega')] = \delta(\omega + \omega')$.

It is useful now to utilize Eqs. (2.12) and (3.3) to define *stochastic* quadrature variables $X^\theta(\omega)$, with a spectrum of $S(\theta,\omega)$:

$$S(\theta,\omega) = \frac{2\pi}{T}\langle X^\theta(-\omega)X^\theta(\omega)\rangle \ , \tag{3.17a}$$

where we include the output coupler transmissivity κ_j' so that

$$X^\theta(\omega) = \sum_j |\nu|_j (2\kappa_j')^{1/2}[\alpha_j(\omega + \omega_0 - \omega_j^0)e^{i\theta_j} + \alpha_j^\dagger(\omega - \omega_0 + \omega_j^0)e^{-i\theta_j}] \ ,$$

$$\alpha_j(\omega) = \frac{1}{(2\pi)^{1/2}} \int e^{i\omega t}\alpha_j(t) dt \ .$$

Provided the input fields to the relevant mode are in the vacuum state, the stochastic variable correlations correspond directly to a normally ordered operator product of external fields. It is clear from Eq. (3.16) that $S(\theta,\omega)$ which gives a normally ordered variance, indicates the extent of nonclassical statistical behavior:

$$V(\theta,\omega) = 1 + S(\theta,\omega) \ . \tag{3.17b}$$

Using this normally ordered form, which is valid even for $|\nu_j| \neq 1$, $V(\theta,\omega)$ can now be related directly to stochastic correlation functions of the internal variables $\alpha, \alpha^\dagger$.

We first define a generalized spectrum $s_{ij}(\omega)$ and cross-correlation spectrum $c_{ij}(\omega)$. These only refer to intracavity correlations, but include the damping rates κ_1^0 for purposes of normalization:

$$s_{ij}(\omega) = 2(\kappa_i^0\kappa_j^0)^{1/2} \int \langle :\hat{a}_i^\dagger(0)\hat{a}_j(\tau):\rangle e^{i\omega\tau} d\tau \ ,$$
$$c_{ij}(\omega) = 2(\kappa_i^0\kappa_j^0)^{1/2} \int \langle :\hat{a}_i(0)\hat{a}_j(\tau):\rangle e^{i\omega\tau} d\tau \ . \tag{3.18}$$

This can be readily simplified to an expectation value of Fourier transforms, in a generalized Wiener-Khintchine theorem. In terms of stochastic variables

$$s_{ij}(\omega) = \frac{4\pi(\kappa_i^0\kappa_j^0)^{1/2}}{T}\langle \alpha_i^\dagger(-\omega)\alpha_j(\omega)\rangle \ ,$$
$$c_{ij}(\omega) = \frac{4\pi(\kappa_i^0\kappa_j^0)^{1/2}}{T}\langle \alpha_i(-\omega)\alpha_j(\omega)\rangle \ . \tag{3.19}$$

Next we use the input-output relationships [Eq. (3.3)] to relate $s(\omega)$ and $c(\omega)$ to the external modes:

$$s_{ij}(\omega) = \frac{1}{T}\left[\frac{\kappa_i^0\kappa_j^0}{\kappa_i^1\kappa_j^1}\right]^{1/2} \times \int\int \langle [\hat{\Phi}_i^{\text{out}}(t)]^\dagger \hat{\Phi}_j^{\text{out}}(t+\tau)\rangle \times \exp[-i(\omega + \omega_i^0)t + i(\omega + \omega_j^0)(t+\tau)] dt\, d\tau \ ,$$
$$c_{ij}(\omega) = \frac{1}{T}\left[\frac{\kappa_i^0\kappa_j^0}{\kappa_i^1\kappa_j^1}\right]^{1/2} \times \int\int \langle \hat{\Phi}_i^{\text{out}}(t)\hat{\Phi}_j^{\text{out}}(t+\tau)\rangle \times \exp[-i(\omega - \omega_i^0)t + i(\omega + \omega_j^0)(t+\tau)] dt\, d\tau \ . \tag{3.20}$$

As we will calculate the intracavity correlation functions and $s(\omega)$ and $c(\omega)$, in the following sections, it is useful to reexpress the squeezing variance $V(\theta,\omega)$ in terms of these quantities. Keeping only the terms of the form $\langle \alpha_i(-\omega)\alpha_j(\omega)\rangle$ (for $i \neq j$) and $\langle \alpha_i^\dagger(-\omega)a_j(\omega)\rangle$ (for $i = j$)—since we will find later that other terms all vanish identically—the variance is calculated to be

$$V(\theta,\omega) = 1 + \eta_1[s_{11}(\omega - \epsilon) + s_{11}(-\omega + \epsilon)] + \eta_2[s_{22}(\omega + \epsilon) + s_{22}(\omega - \epsilon)] + 2\sqrt{\eta_1\eta_2}\,\text{Re}\{e^{2i\theta}[c_{12}(\omega + \epsilon) + c_{21}(\omega - \epsilon)]\} \ ,$$

where (3.21)

$$2\theta=\theta_1+\theta_2 ,$$

$$\eta_i=|\nu_i|^2\kappa_i/\kappa_i^0 .$$

We have not included terms such as s_{33} and c_{33} involving the pump mode α_3 since these are significant only near zero frequency, $\omega=0$. The expression $V(\theta,\omega)$ is thus similar to the "two-mode squeezing" spectrum considered originally by Caves and Schumaker.[23] The factors η_i are overall efficiency factors that account for both intracavity and extracavity absorption or losses, as well as for the photodetector efficiency.

We see here that the phase dependence occurs only through $\theta=\frac{1}{2}(\theta_1+\theta_2)$. This is a general expression that principally assumes a time-invariant steady state in the two modes. It also implicitly assumes that the two modes are nonoverlapping in frequency, so that the spectral width of each of $s(\omega)$ and $c(\omega)$ are much less than ϵ, and that (as is the case throughout this paper) $s_{12}(\omega)=s_{21}(\omega)=c_{11}(\omega)=c_{22}(\omega)=0$. In the equal-efficiency case of $\eta_1=\eta_2=\eta$, we can also write

$$V(\theta,\omega)=1+[S^{(1)}(\theta,\omega-\epsilon)+S^{(1)}(\theta,-\omega-\epsilon)] , \tag{3.22}$$

where [noting that $c_{12}(\omega)=c_{21}(-\omega)$ identically] we have divided $S(\theta,\omega)$ into two symmetric parts, with

$$S^{(1)}(\theta,\omega)=\eta\{s_{11}(\omega)+s_{22}(-\omega) +2\,\mathrm{Re}[e^{2i\theta}c_{21}(\omega)]\} . \tag{3.23}$$

The quantity $S^{(1)}(\theta,\omega)$ is a direct indicator of the extent of squeezing. When $S^{(1)}$ has negative values, the field is nonclassical, and squeezing has occurred. The largest degree of squeezing is for $S^{(1)}=-1$. We note that the total measured variance V is symmetric in frequency around $\omega=0$. On the other hand, $S^{(1)}$ may not be exactly symmetric around $\omega=0$. The observed variance V can only reach its minimum value of $V=0$ at the spectral locations where $S^{(1)}=-1$. As the two modes are nonoverlapping, the two spectral terms in Eq. (3.22) cannot both equal -1 simultaneously. Thus $V=0$ can only occur for perfect overall efficiency, i.e., $\eta=1$. Of course, in the limit of complete noise reduction, the other quadrature will have infinitely large fluctuations.

We note that in experiments it is sometimes useful to arrange the detection apparatus differently from that shown in Fig. 1. It is common to use a 50-50 beam splitter, and to detect the difference current between the two resulting output beams. This is known as balanced homodyne detection. For simplicity, we do not treat this case in detail. The result of the balanced homodyne scheme is the complete suppression of the coherent term proportional to $\delta(\omega)$, provided that two arms of the beam-splitter output are exactly matched.

B. Twin-local-oscillator case

Next we shall consider the class of squeezing experiments in which the two output beams have distinct local oscillators, as shown in Fig. 2. In this category are included experiments with modes of orthogonal polarization, since the signal and idler beams then interfere with distinct and independent polarizations of the local oscillator. In the general case there are two photon fluxes, $\hat{I}_1$ and $\hat{I}_2$. A number of cross correlations can be calculated, together with their corresponding current spectra, i.e.,

$$G_{ij}^{(2)}(t,t')=\langle :\hat{I}_i(t)\hat{I}_j(t'):\rangle . \tag{3.24}$$

The corresponding current cross-correlation spectum is

$$G_{ij}^{I}(\omega)=Z_iZ_je^2\left[\delta_{ij}\langle\hat{I}_j(0)\rangle+\int e^{i\omega\tau}G_{ij}^{(2)}(0,\tau)d\tau\right] . \tag{3.25}$$

Here the current correlation function is calculated following precisely the arguments of (3.8)–(3.12). The local oscillators can in general now have arbitrary frequencies. However, we will use the optimal choice, which is that the local-oscillator frequencies correspond to the two mode frequencies ω_1^0 and ω_2^0.

We can now calculate the cross-spectral current correlations directly in terms of quadrature correlations, as before. In the limit of intense local oscillators

$$\frac{G_{ij}^{I}(\omega)}{Z_iZ_je^2}=\delta_{ij}\delta(\omega)(I_i^0+I_i^s)^2 +(I_i^0I_j^0)^{1/2}\left[\delta_{ij}+\frac{2\pi}{T}\langle :\hat{X}_i^{\theta_i}(-\omega)\hat{X}_j^{\theta_j}(\omega):\rangle\right] , \tag{3.26}$$

where

$$\hat{X}_j^{\theta_j}(\omega)=\frac{1}{\sqrt{2\pi}}\int e^{i\omega t}\hat{X}_j^{\theta_j}(t)dt ,$$

$$\hat{X}_j^{\theta_j}(t)=|\nu_j|e^{i(\theta_j+\omega_j^0t)}\hat{\Phi}_j^{\mathrm{out}}(t)+\mathrm{H.c.}$$

This leads to the obvious definition of the normalized cross-spectral variance:

$$V_{ij}(\theta_1,\theta_2,\omega)=\delta_{ij}+S_{ij}(\theta_1,\theta_2,\omega) ,$$

where

$$S_{ij}(\theta_1,\theta_2,\omega)=\frac{2\pi}{T}\langle :\hat{X}_i^{\theta_i}(-\omega)\hat{X}_j^{\theta_j}(\omega):\rangle . \tag{3.27}$$

Once again, as in the earlier case, for perfect efficiency this reduces to a non-normally ordered operator product:

$$V_{ij}(\theta_1,\theta_2,\omega)=\frac{2\pi}{T}\langle[\hat{X}_i^{\theta_i}(\omega)]^{\dagger}[\hat{X}_j^{\theta_j}(\omega)]\rangle . \tag{3.28}$$

The normally ordered spectral covariance $S_{ij}(\theta_1,\theta_2,\omega)$ can be regarded as the measure of the departure from classical statistics, since the *normally* ordered expectation values behave as classical averages when the fields have classical statistics.

It is useful to express the normally ordered spectral covariance in terms of the spectral matrices $s(\omega)$ and $c(\omega)$, as in the earlier case. We find that

$$S_{ij}(\theta_1,\theta_2,\omega)=\{s_{ij}(\omega)+s_{ji}(-\omega)+c_{ij}(\omega)e^{i(\theta_i+\theta_2)} +[c_{ji}(\omega)]^*e^{-i(\theta_1+\theta_2)}\} . \tag{3.29}$$

In the case of the parametric oscillator, we have

$s_{12}(\omega)=s_{21}(\omega)=c_{11}(\omega)=c_{22}(\omega)=0$, so that

$$S_{jj}(\theta_j,\theta_j,\omega)=s_{jj}(\omega)+s_{jj}(-\omega)\ ,$$
$$S_{12}(\theta_1,\theta_2,\omega)=c_{12}(\omega)e^{i(\theta_1+\theta_2)}+[c_{21}(\omega)]^*e^{-i(\theta_1+\theta_2)}\ . \tag{3.30}$$

Of most interest in the present paper will be the current-fluctuation spectrum in the two current combinations: $i_\pm=i_1\pm i_2$. It is useful to define additional two-time correlation functions in terms of G_{ij} that can be written

$$\begin{aligned}G^{(2)}_{(+)}(t,t')&=G^{(2)}_{11}(t,t')+(Z_2/Z_1)^2G^{(2)}_{22}(t,t')\\&\quad+(Z_2/Z_1)[G^{(2)}_{12}(t,t')+G^{(2)}_{21}(t,t')]\ ,\\G^{(2)}_{(-)}(t,t')&=G^{(2)}_{11}(t,t')+(Z_2/Z_1)^2G^{(2)}_{22}(t,t')\\&\quad-(Z_2/Z_1)[G^{(2)}_{12}(t,t')+G^{(2)}_{21}(t,t')]\ .\end{aligned} \tag{3.31}$$

It is clear from Eq. (3.26) that the shot-noise contribution to the current spectrum is $(Z_1^2I_1^0+Z_2^2I_2^0)e^2$. Hence the combination photocurrent spectra will be, after Fourier transforming and dropping terms in the shot noise of order I^s,

$$\frac{G^I_\pm(\omega)}{(Z_1e)^2}=I_1^0+I_2^0(Z_2/Z_1)^2+\int e^{i\omega\tau}\{G^{(2)}_{11}(0,\tau)+(Z_2/Z_1)^2G^{(2)}_{22}(0,\tau)\pm(Z_2/Z_1)[G^{(2)}_{12}(0,\tau)+G^{(2)}_{21}(0,\tau)]\}d\tau\ . \tag{3.32}$$

The result for the photocurrent spectra is then

$$\frac{G^I_\pm(\omega)}{(Z_1e)^2}=[I_1^0+I_1^s\pm(Z_2/Z_1)(I_2^0+I_2^s)]^2\delta(\omega)+I_1^{(0)}(1+g^2)+I_1^0\int e^{i\omega\tau}\langle:[\hat{X}^{\theta_1}_1(0)\pm g\hat{X}^{\theta_2}_2(0)][\hat{X}^{\theta_1}_1(\tau)\pm g\hat{X}^{\theta_2}_2(\tau)]:\rangle d\tau\ , \tag{3.33}$$

where

$$g=(Z_2/Z_1)(I_2^0/I_1^0)^{1/2}\ .$$

Here g can be thought of as the relative gain of the channel-two detector compared to the channel-one detector.

Just as before, it is appropriate to define a squeezing variance that is positive definite and equal to unity in the vacuum or coherent signal case. This is given, after subtracting the coherent (δ-function) component, by normalizing with the shot-noise power spectrum:

$$\begin{aligned}V_\pm(\theta_1,\theta_2,\omega)&=1+2\eta\,\mathrm{Re}(s_{11}(\omega)+g^2s_{22}(\omega)\\&\quad\pm g\{\exp[i(\theta_1+\theta_2)]\}\\&\quad\times[c_{12}(\omega)+c_{21}(\omega)])/(1+g^2)\\&=1+S_\pm(\theta_1,\theta_2,\omega)\ ,\end{aligned} \tag{3.34}$$

where

$$S_\pm(\theta_1,\theta_2\omega)=\frac{2\pi}{T}\langle:\hat{X}_\pm(-\omega)\hat{X}_\pm(+\omega):\rangle,$$
$$\hat{X}_\pm(\omega)=[\hat{X}^{\theta_1}_1(\omega)\pm g\hat{X}^{\theta_2}_2(\omega)]/(1+g^2)^{1/2}\ .$$

Here we have utilized the vanishing of $s_{12}(\omega)$, $s_{21}(\omega)$, $c_{22}(\omega)$, and $c_{11}(\omega)$, and assumed that $\eta_1=\eta_2$ to simplify the expression for later applications. The detector efficiency η is defined as in Eq. (3.21).

The following equalities are easily obtained in the case $g=1$, providing $s_{jj}(\omega)=s_{jj}(-\omega)$ and $c_{ij}(\omega)=c_{ij}(-\omega)$:

$$\begin{aligned}S_+(\theta_1,\theta_2,\omega)&=S^{(1)}(\theta_1+\theta_2,\omega)\ ,\\S_-(\theta_1,\theta_2,\omega)&=S^{(1)}(\pi+\theta_1+\theta_2,\omega)\ .\end{aligned} \tag{3.35}$$

Thus in the special case treated here, there is a direct relationship between the single-oscillator variances and the double-oscillator variances characteristic of twin-output experiments. We shall calculate $V(\theta,\omega)$ explicitly in Sec. VI. A discussion of the physical implications of the two-mode experiments is given in Sec. VII and VIII.

We note that there is a clear physical distinction between the single-local oscillator and the double-local-oscillator types of squeezing measurement. The single-local-oscillator measurement, which is applicable to a nondegenerate signal-idler frequency, produces a twin spectrum with no squeezing near zero frequency. The double-local-oscillator measurement is best made with local oscillators individually resonant with the relevant modes, thus producing a spectrum near zero frequency. If nonresonant local oscillators are used in the double-local-oscillator experiment—or, equivalently, if orthogonal polarizations with nondegenerate frequencies are used in a single-local-oscillator experiment—a twin spectrum is predicted, but with a maximum squeezing of only 50%.

We finally comment on the types of nonclassical behavior that can be found in these twin-beam experiments. It is useful to define rigorously what we mean by classical statistical behavior. The simplest definition is that a classical field is one generated by a classical macroscopic current source. This corresponds to a coherent state in quantum field theory. Of course, this must be generalized to include classical statistical mixtures, which are represented by the use of a positive, diagonal P distribution. Thus, classical behavior in a correlation measurement corresponds to a field either in a coherent state or having a positive Glauber-Sudarshan[19,33] P representation. This implies that all normally ordered variances are positive. In single-mode experiments the criteria that are most commonly used for classical statistics are that there is neither photon antibunching nor squeezing. In our notation, this implies that, for all phase angles θ,

$$S(\theta,\omega)\geq 0 \ . \tag{3.36}$$

We note that in the case of an experiment *without* a local oscillator, the corresponding inequality for classical photon statistics is[34]

$$G^{(2)}(\omega)\geq 0 \ . \tag{3.37}$$

Violation of this inequality corresponds to photon antibunching. For an experiment with two local oscillators, a larger number of conditions can occur. The most obvious of these is the counterpart to the antibunching criterion, i.e., for classical photon statistics,

$$G^{(2)}_{\pm}(\omega)\geq 0 \ . \tag{3.38}$$

We can now obtain some relationships that are unique to the two-mode experiment. First of all, we note that since $\hat{X}_j(-\omega)=[\hat{X}_j(\omega)]^{\dagger}$, we must have, for any complex gain $\tilde{g}$,

$$\langle[\hat{X}_i(-\omega)+\tilde{g}^*\hat{X}_j(-\omega)][\hat{X}_i(\omega)+\tilde{g}\hat{X}_j(\omega)]\rangle\geq 0 \ . \tag{3.39}$$

Here we drop the angular argument $[\theta_i]$ for simplicity. The term $\tilde{g}$ has arbitrary phase and will be chosen so that

$$\langle\tilde{g}^*\hat{X}_j(-\omega)X_i(\omega)+\tilde{g}\hat{X}_i(-\omega)\hat{X}_j(\omega)\rangle = -2|\tilde{g}\langle\hat{X}_i(-\omega)\hat{X}_j(\omega)\rangle| \ . \tag{3.40}$$

Rearranging and choosing:

$$|\tilde{g}|=|\langle\hat{X}_i(-\omega)\hat{X}_j(\omega)\rangle|/|\langle\hat{X}_j(-\omega)\hat{X}_j(\omega)\rangle| \ , \tag{3.41}$$

we have the general result that

$$\langle\hat{X}_i(-\omega)\hat{X}_i(\omega)\rangle\langle\hat{X}_j(-\omega)\hat{X}_j(\omega)\rangle\geq|\langle\hat{X}_i(-\omega)\hat{X}_j(\omega)\rangle|^2 \ . \tag{3.42}$$

This results in a quantum Cauchy-Schwarz inequality. For perfectly efficient detectors, using the earlier notation, we obtain a relationship between the observed variances:

$$V_{ii}(\theta_1,\omega)V_{jj}(\theta_2,\omega)\geq|V_{ij}(\theta_1,\theta_2,\omega)|^2 \ , \tag{3.43}$$

where

$$V_{ij}(\theta_i,\theta_j,\omega)=\frac{2\pi}{T}\langle\hat{X}_i(-\omega)\hat{X}_j(\omega)\rangle \ .$$

However, similar classical arguments can be utilized for the case of a classical field with a Glauber-Sudarshan positive P distribution. In this case, we use the stochastic representation of $\hat{X}$ and note that for the case of diagonal coherent state expansion, one must have $X(-\omega)=X(\omega)$ for each stochastic path. The corresponding operator correlations are, of course, the normally ordered correlations. Hence we obtain, for classical fields,

$$\langle:\hat{X}_i(-\omega)\hat{X}_i(\omega):\rangle\langle\hat{X}_j(-\omega)\hat{X}_j(\omega):\rangle \geq|\langle:\hat{X}_i(-\omega)\hat{X}_j(\omega):\rangle|^2 \ , \tag{3.44}$$

which implies that

$$S_{ii}(\theta_1,\omega)S_{jj}(\theta_2,\omega)\geq|S_{ij}(\theta_1,\theta_2,\omega)|^2 \ , \tag{3.45}$$

where, just as before,

$$S_{ij}(\theta_i,\theta_j,\omega)=\frac{2\pi}{T}\langle:\hat{X}_i(-\omega)\hat{X}_j(\omega):\rangle \ .$$

This inequality can be violated by fields with quantum correlations, even though the earlier inequality is satisfied. The extent of violation of the classical inequality is maximized for perfect detectors. We use the obvious relations that

$$\begin{aligned} &V_{ii}(\theta_i,\omega)=1+S_{ii}(\theta_i,\omega) \\ &V_{ij}(\theta_i,\theta_j,\omega)=S_{ij}(\theta_i,\theta_j,\omega), \quad i\neq j \ . \end{aligned} \tag{3.46}$$

Hence, the normalized cross-correlation function S_{12} is strictly bounded by

$$|S_{12}(\theta_1,\theta_2,\omega)|^2\leq[1+S_{11}(\theta_1,\omega)][1+S_{22}(\theta_2,\omega)] \ . \tag{3.47}$$

In all the cases treated in this paper, we have the identities $s_{12}(\omega)=s_{21}(\omega)=c_{22}(\omega)=c_{11}(\omega)=0$. Thus the results of Eq. (3.30) can be utilized to give the classical Cauchy-Schwarz inequality as

$$|c_{12}(\omega)e^{i(\theta_1+\theta_2)}+[c_{21}(\omega)]^*e^{-i(\theta_1+\theta_2)}|^2 \leq\prod_{j=1}^{2}[s_{jj}(\omega)+s_{jj}(-\omega)] \ . \tag{3.48}$$

Violation of this inequality is a situation where there is a greater than classical correlation between quadrature phases, and it is clear that this violation of classical statistics is permitted by the strict quantum-theoretic bound of Eq. (3.47).

The violation of this inequality is a generalized type of squeezing. This can lead to situations of the type envisaged by Einstein, Podolsky, and Rosen[28] in their work on the EPR paradox. These situations will be treated in more detail in Sec. VIII.

IV. SEMICLASSICAL RESULTS

We now proceed to analyze and to solve the stochastic equations (2.11) describing the parametric oscillator. The semiclassical properties of the above equations are discussed in detail in some earlier papers.[14,15] These well-known results are reproduced here in our notation, for completeness. In contrast to most earlier works, however, we keep the results quite general by allowing for nonequal decay rates κ_j and nonzero detuning Δ_j.

It is clear that the steady-state amplitudes of α_i^0 are obtained on setting $\partial_t\alpha_i=0=\zeta_i(t)$ in Eq. (2.11). Solving for the signal and idler modes,

$$\alpha_1^0=g\alpha_3^0\alpha_2^0/\kappa_1 \ ,$$

and

$$\alpha_2^0=g\alpha_3^0\alpha_1^0/\kappa_2 \ . \tag{4.1}$$

This implies that either

$$\alpha_1^0=(\alpha_1^0)^{\dagger}=\alpha_2^0=(\alpha_2^0)^{\dagger}=0$$

or

$$g^2\alpha_3^0(\alpha_3^0)^{\dagger}=\kappa_1\kappa_2^* \ . \tag{4.2}$$

In the semiclassical limit, we will only consider steady-state solutions in which $(\alpha_3^0)^*=(\alpha_3^0)^\dagger$, as these correspond to classical fields. Thus the solutions fall into two categories at all input powers. The first solution is immediate, and gives the below-threshold behavior:

$$\alpha_1^0=0\ ,\quad \alpha_2^0=0\ ,\quad \alpha_3^0=E/\kappa_3\ , \tag{4.3}$$

In the above-threshold case, the condition $(\alpha^0)^*=(\alpha^0)^\dagger$ implies that $\kappa_1\kappa_2^*$ must be real. Thus any detuning present in the signal and idler modes is necessarily proportional to the cavity decay rates, or else only limit-cycle-type behavior can occur in the above-threshold solutions. This symmetric choice is always possible since $\omega_1^0-\omega_2^0$ is arbitrary, as stated earlier. The field amplitudes can be written in terms of their phase and intensity as follows:

$$\alpha_j=(\alpha_j^\dagger)^*=I_j^{1/2}\exp(-i\phi_j)\ ,\quad E=|E|\exp(-i\phi_0)\ . \tag{4.4}$$

It is clear from Eq. (2.11) that for the steady state

$$|E|e^{-i\phi_0}-g^{-1}\kappa_3(\kappa_1\kappa_2^*)^{1/2}e^{-i\phi_3}-g|\alpha_1^0\alpha_2^0|e^{-i(\phi_1+\phi_2)}=0\ . \tag{4.5}$$

But Eq. (4.1) gives a relationship between α_1^0 and α_2^0; hence, for the steady state

$$|\alpha_1|=\frac{(\kappa_1\kappa_2^*)^{1/2}}{|\kappa_1|},\quad \text{and}\quad e^{-i(\phi_2+\phi_1)}=\frac{\kappa_1^*}{|\kappa_1|}e^{-i\phi_3}\ . \tag{4.6}$$

Upon inserting the phase relation into (4.5), the resulting complex equation allows us to solve for the steady-state, above-threshold values of $\phi_3-\phi_0$ and $\bar{I}=|\alpha_1^0||\alpha_2^0|$. We find from the imaginary part of Eq. (4.5) that

$$\tan(\theta_3-\theta_0)=\frac{\Delta_3(\kappa_1\kappa_2^*)^{1/2}/g-g\bar{I}\Delta_1/|\kappa_1|}{\kappa_3^0(\kappa_1\kappa_2^*)^{1/2}/g+g\bar{I}\kappa_1^0/|\kappa_1|}\ . \tag{4.7}$$

Substitution back into the real part of (4.5) and examination of the limit $\bar{I}\to 0$ allow us to deduce the existence of at least one above-threshold solution (requiring $\bar{I}>0$) as the driving field amplitude E increases in magnitude above a threshold amplitude E_T. The threshold amplitude is given by $E_T=|\kappa_3|(\kappa_1\kappa_2^*)^{1/2}/g$. In the present paper we restrict our attention to the below-threshold solutions, $|E|<E_T$. The above-threshold solutions and fluctuations were examined in the earlier paper.[18]

V. LINEARIZED EQUATIONS AND SOLUTIONS BELOW THRESHOLD

We now analyze the below-threshold behavior with $|E|<E_T$, by linearizing the equations (2.11) about the steady-state semiclassical result: $\alpha_1^0=\alpha_2^0=0$, $\alpha_3^0=E/\kappa_3$. Below-threshold solutions have been obtained in previous works[15,16] in the limit of equal decay rates and zero detunings. We will show that the steady-state solutions are stable. Hence we may solve Eqs. (2.11) below threshold to a good approximation by the linearization procedure, which assumes small fluctuations $\Delta\alpha_j=\alpha_j-\alpha_j^0$ about the steady state. The linearized equations are

$$\begin{aligned}
\partial_t\Delta\alpha_1&=-\kappa_1\Delta\alpha_1+g\alpha_3^0\Delta\alpha_2^\dagger+F_1(t)\ ,\\
\partial_t\Delta\alpha_2&=-\kappa_2\Delta\alpha_2+g\alpha_3^0\Delta\alpha_1^\dagger+F_2(t)\ ,\\
\partial_t\Delta\alpha_3&=-\kappa_3\Delta\alpha_3\ ,\\
\partial_t\Delta\alpha_1^\dagger&=-\kappa_1^*\Delta\alpha_1^\dagger+g\alpha_3^{0*}\Delta\alpha_2^\dagger+F_1^\dagger(t)\ ,\\
\partial_t\Delta\alpha_2^\dagger&=-\kappa_2^*\Delta\alpha_2^\dagger+g\alpha_3^{0*}\Delta\alpha_1^\dagger+F_2^\dagger(t)\ ,\\
\partial_t\Delta\alpha_3^\dagger&=-\kappa_3^*\Delta\alpha_3^\dagger\ .
\end{aligned} \tag{5.1}$$

The nonzero steady-state noise correlations in this small-noise approximation are

$$\langle F_1(t)F_2(t')\rangle=g\frac{|E|}{\kappa_3}\delta(t-t')\ ,\quad \langle F_1^\dagger(t)F_2^\dagger(t')\rangle=g\frac{|E|}{\kappa_3^*}\delta(t-t')\ .$$

We note immediately that below threshold the pump fluctuations $\Delta\alpha_3,\Delta\alpha_3^\dagger$ always decouple from the signal and idler fluctuations. In fact, $\Delta\alpha_3=0$ in the steady state, indicating that in this linearization procedure the coherent input field produces a coherent pump mode in the cavity. The signal and idler modes have quantum fluctuations, which we shall calculate in the remainder of this section. We use the notation α_j instead of $\Delta\alpha_j$ for $j=1,2$ from now on for simplicity, because $\alpha_j=\Delta\alpha_j$ in these cases. We note that the linearization procedure is valid for small fluctuations and does not hold in the critical region near $E=E_T$.

We write the deterministic signal and idler equations of Eq. (5.1) as $\partial_t\boldsymbol{\alpha}=-\mathsf{A}\cdot\boldsymbol{\alpha}$, where $\boldsymbol{\alpha}=(\alpha_1,\alpha_2,\alpha_1^\dagger,\alpha_2^\dagger)$. The eigenvalues of the deterministic part of the signal and idler equations are readily found to be

$$\lambda_{1,2}=\frac{\kappa_1^0+\kappa_2^0}{2}+i\frac{\Delta_1-\Delta_2}{2}\pm\tfrac{1}{2}(x_++ix_-)\ ,\quad \lambda_{3,4}=\lambda_{1,2}^*\ , \tag{5.2}$$

where

$$x_\pm=[\pm c/2+\tfrac{1}{2}(c^2+d^2)^{1/2}]^{1/2}$$

and

$$c=(\kappa_1^0-\kappa_2^0)^2-(\Delta_1+\Delta_2)^2+4g^2|E|^2/|\kappa_3|^2\ ,\quad d=2(\kappa_1^0-\kappa_2^0)(\Delta_1+\Delta_2)\ .$$

The linearized equations (and hence the steady-state solution) are stable where the real parts of all the eigenvalues are positive. Thus for stability we require $\kappa_1^0+\kappa_2^0>x_+$. A little algebra reveals that the steady-state, below-threshold solutions (4.3) are stable where $|E|<E_T$. Thus, fluctuations from the steady-state deterministic solution are damped before becoming too large (provided we are not too close to threshold) and the linearization procedure is valid. Above threshold

($|E| > E_T$) the solutions (4.3) are unstable.

Since we are primarily interested in spectra, Eqs. (5.1) are most conveniently solved by transformation into frequency space. We define the following Fourier-transformed variables:

$$\begin{aligned}
\alpha_j(\omega)&=\frac{1}{\sqrt{2\pi}}\int_{-\infty}^{\infty}e^{i\omega t}\alpha_j(t)dt\ ,\\
\alpha_j^{\dagger}(\omega)&=\frac{1}{\sqrt{2\pi}}\int_{-\infty}^{\infty}e^{i\omega t}\alpha_j^{\dagger}(t)dt\ ,\\
F_j(\omega)&=\frac{1}{\sqrt{2\pi}}\int_{-\infty}^{\infty}e^{i\omega t}F_j(t)dt\ ,\\
F_j^{\dagger}(\omega)&=\frac{1}{\sqrt{2\pi}}\int_{-\infty}^{\infty}e^{i\omega t}F_j^{\dagger}(t)dt\ .
\end{aligned}\tag{5.3}$$

The nonzero noise correlations in frequency space are readily calculated from these definitions, as

$$\begin{aligned}
\langle F_1(\omega)F_2(\omega')&=(gE/\kappa_3)\delta(\omega+\omega')\ ,\\
\langle F_1^{\dagger}(\omega)F_2^{\dagger}(\omega')&=(gE/\kappa_3^{*})\delta(\omega+\omega')\ .
\end{aligned}$$

On converting Eqs. (5.1) into frequency space, we obtain the following set of algebraic equations which are then readily solved:

$$\begin{aligned}
0&=(i\omega-\kappa_1)\alpha_1(\omega)+g\alpha_3^0\alpha_2^{\dagger}(\omega)+F_1(\omega)\ ,\\
0&=(i\omega-\kappa_2)\alpha_2(\omega)+g\alpha_3^0\alpha_1^{\dagger}(\omega)+F_2(\omega)\ ,\\
0&=(i\omega-\kappa_1^{*})\alpha_1^{\dagger}(\omega)+g(\alpha_3^0)^{*}\alpha_2(\omega)+F_1^{\dagger}(\omega)\ ,\\
0&=(i\omega-\kappa_2^{*})\alpha_2^{\dagger}(\omega)+g(\alpha_3^0)^{*}\alpha_1(\omega)+F_2^{\dagger}(\omega)\ .
\end{aligned}\tag{5.4}$$

The solutions are

$$\begin{aligned}
\alpha_1(\omega)&=\frac{g\alpha_3^0F_2^{\dagger}(\omega)-(i\omega-\kappa_2^{*})F_1(\omega)}{(i\omega-\kappa_2^{*})(i\omega-\kappa_1)-g^2|\alpha_3^0|^2}\ ,\\
\alpha_2^{\dagger}(\omega)&=\frac{g\alpha_3^{0*}F_1(\omega)-(i\omega-\kappa_1)F_2^{\dagger}(\omega)}{(i\omega-\kappa_1)(i\omega-\kappa_2^{*})-g^2|\alpha_3^0|^2}\ ,\\
\alpha_2(\omega)&=\frac{g\alpha_3^0F_1^{\dagger}(\omega)-(i\omega-\kappa_1^{*})F_2(\omega)}{(i\omega-\kappa_1^{*})(i\omega-\kappa_2)-g^2|\alpha_3^0|^2}\ ,\\
\alpha_1^{\dagger}(\omega)&=\frac{g\alpha_3^{0*}F_2(\omega)-(i\omega-\kappa_2)F_1^{\dagger}(\omega)}{(i\omega-\kappa_2)(i\omega-\kappa_1^{*})-g^2|\alpha_3^0|^2}\ .
\end{aligned}\tag{5.5}$$

We are particularly interested in the steady-state quantities $s_{ij}(\omega)$ and $c_{ij}(\omega)$ defined by Eq. (3.19). Using the definition of the inverse Fourier transform,

$$\alpha_j(t)=\frac{1}{\sqrt{2\pi}}\int_{-\infty}^{\infty}\alpha_j(\omega)e^{-i\omega t}d\omega\tag{5.6}$$

and the properties of the δ function, it is straightforward to show that

$$\begin{aligned}
\langle\alpha_i(\omega')\alpha_j(\omega)\rangle&=\left[\frac{c_{ij}(\omega)}{2(\kappa_i^0\kappa_j^0)^{1/2}}\right]\delta(\omega+\omega')\ ,\\
\langle\alpha_i^{\dagger}(\omega')\alpha_j(\omega)\rangle&=\left[\frac{s_{ij}(\omega)}{2(\kappa_i^0\kappa_j^0)^{1/2}}\right]\delta(\omega+\omega')\ ,
\end{aligned}\tag{5.7}$$

in accordance with Eq. (3.20). Hence the spectra are readily calculated from (5.5). We find that

$$c_{11}(\omega)=c_{22}(\omega)=s_{21}(\omega)=s_{12}(\omega)=0\ .\tag{5.8}$$

Our central theoretical result is for the nonzero elements, which are

$$\begin{aligned}
s_{11}(\omega)=s_{22}(-\omega)&=\frac{4\kappa_1^0\kappa_2^0g^2|\alpha_3^0|^2}{|(i\omega-\kappa_2^{*})(i\omega-\kappa_1)-g^2|\alpha_3^0|^2|^2}\ ,\\
c_{21}(\omega)=c_{12}(\omega)&=\frac{2(\kappa_1^0\kappa_2^0)^{1/2}g\alpha_3^0[g^2|\alpha_3^0|^2+(i\omega-\kappa_2^{*})(-i\omega-\kappa_1^{*})]}{|(i\omega-\kappa_2^{*})(i\omega-\kappa_1)-g^2|\alpha_3^0|^2|^2}\ .
\end{aligned}\tag{5.9}$$

The solutions are a function of the following scaled variables:

$$\bar{\omega}=\frac{\omega}{(\kappa_1^0\kappa_2^0)^{1/2}},\quad P=\frac{|E|}{E_T},\quad \bar{\Delta}=\frac{\Delta_i}{\kappa_i^0},\quad r=\frac{\kappa_2^0}{\kappa_1^0}\ .\tag{5.10}$$

For the case of symmetric decay rates ($\kappa_1^0=\kappa_2^0=\kappa^0$) and zero detunings, the solutions may be written for the intensity spectra as

$$s_{11}(\omega)=s_{22}(\omega)=P\left[\frac{1}{(1-P)^2+\bar{\omega}^2}-\frac{1}{(1+P)^2+\bar{\omega}^2}\right]\ .\tag{5.11}$$

The cross-correlation spectra then are given by

$$c_{21}(\omega)=c_{12}(\omega)=P\left[\frac{1}{(1-P)^2+\bar{\omega}^2}+\frac{1}{(1+P)^2+\bar{\omega}^2}\right]\ .\tag{5.12}$$

The direct intensity spectrum $s_{11}(\omega)$ associated with mode $\hat{a}_1$ is the sum of two Lorentzians, centered at $\omega=0$ and with widths $2\kappa^0(1-P)$ and $2\kappa^0(1+P)$. We note the divergence in the first Lorentzian as threshold is approached ($P\rightarrow 1$).

One may now calculate the various squeezing spectra discussed in Sec. III. The results obtained in this section relate to the intracavity correlations $s_{ij}(\omega)$ and $c_{ij}(\omega)$. In the following sections, we relate these to the external correlation spectra observed using different types of measurements.

VI. SQUEEZING WITH SINGLE LOCAL OSCILLATORS

The case of a single local oscillator gives results that are applicable for a single polarization direction and nondegenerate frequencies. This has been termed "two-mode" squeezing. The "two-mode" squeezing spectrum measured with a single local oscillator takes the form given by (3.22) where ($\epsilon=\omega_1^0-\omega_0=\omega_0-\omega_2^0$)

$$V(\theta,\omega)=1+[S^{(1)}(\theta,\omega-\epsilon)+S^{(1)}(\theta,-\omega-\epsilon)] , \tag{6.1}$$

where

$$S^{(1)}(\theta,\omega)=\eta\{s_{11}(\omega)+s_{22}(-\omega)+2\,\mathrm{Re}[e^{2i\theta}c_{21}(\omega)]\} .$$

For $\theta=\pi/2$, chosen to minimize the noise level $V(\theta,\omega)$, we have

$$S^{(1)}(\pi/2,\omega)=-\frac{4P\eta}{(1+P)^2+\bar{\omega}^2} . \tag{6.2}$$

Thus the observed spectral variance, normalized by the shot noise, will be

$$V(\theta,\omega)=1+\eta\left[\frac{-4P}{(1-P)^2+(\bar{\omega}-\bar{\epsilon})^2}+\frac{-4P}{(1+P)^2+(\bar{\omega}+\bar{\epsilon})^2}\right] , \tag{6.3}$$

where

$$\bar{\epsilon}=\epsilon/\kappa^0 .$$

This gives two minima at $\omega=\pm\epsilon$ in the observed spectrum. It is necessary that $\bar{\epsilon}\gg 1+P$ for the analysis given here to be valid, as we suppose that the two modes decay into uncorrelated reservoirs. For this reason, the two Lorentzian minima are nonoverlapping. As discussed earlier, the case of orthogonal polarizations is treated as having independent local oscillators.

The spectrum localized about each cavity frequency (ω_1^0 or ω_2^0) is thus a negative Lorentzian with width $2\kappa^0(1+P)$ (see Fig. 3). Approaching threshold ($P\to 1$), the noise level $V(\theta,\omega)$ decreases. Total cancellation of shot noise ("perfect squeezing") is obtainable at $\bar{\omega}=\pm\epsilon$ for $\eta=1$. We point out that this linearization procedure will break down near threshold where the fluctuations become larger [one of the eigenvalues (5.2) becomes zero]. We also note as $P\to 1$, the linearized fluctuations in the associated quadrature $\theta=0$ apparently become infinite, though with a narrowing width. In a realistic situation where there is some phase jitter and θ cannot be precisely $\pi/2$, the large fluctuations due to this narrow Lorentzian will tend to reduce squeezing at low frequencies. The optimal squeezing spectrum (6.3) below threshold has an identical shape to that of the degenerate parametric oscillator derived by Collett and Gardiner[12] below threshold, and has been derived by Reynaud *et al.*[16] and Collett and Loudon.[15]

We next consider the effect of asymmetrical decay rates in the absence of detunings ($\bar{\Delta}=0$) on the squeezing spectrum. This is of importance because with nondegenerate modes well separated in frequency it could be difficult to obtain $\kappa_1^0=\kappa_2^0$. First, we point out that the zero frequency ($\bar{\omega}=0$) result is independent of the ratios of decay rates. Thus excellent squeezing still occurs near threshold at $\bar{\omega}=0$ for the quadrature phase $\theta=\pi/2$. In order to examine the case of nonzero $\bar{\omega}$, we note that the optimal squeezing [minimum $S^{(1)}(\theta,\omega)$] is given in general as

$$[S^{(1)}(\theta,\omega)]_{\mathrm{opt}}=s_{11}(\omega)+s_{22}(-\omega)-2|c_{21}(\omega)| , \tag{6.4}$$

where

$$\cos 2\theta=-\frac{\mathrm{Re}[c_{21}(\omega)]}{|c_{12}(\omega)|},\quad \sin 2\theta=\frac{\mathrm{Im}[c_{21}(\omega)]}{|c_{12}(\omega)|} ,$$

and Re and Im denote the real and imaginary parts, respectively. Figure 4 plots this optimal squeezing spectrum for various ratios κ_2^0/κ_1^0 of decay rates in the absence of detunings. We see a still significant squeezing associated with a broad component near threshold. The bandwidth of squeezing, however, is reduced compared to the case $\kappa_1^0=\kappa_2^0$. The optimal phase angle is now frequency dependent, indicating that less squeezing would be observed in an integrated measurement of the total

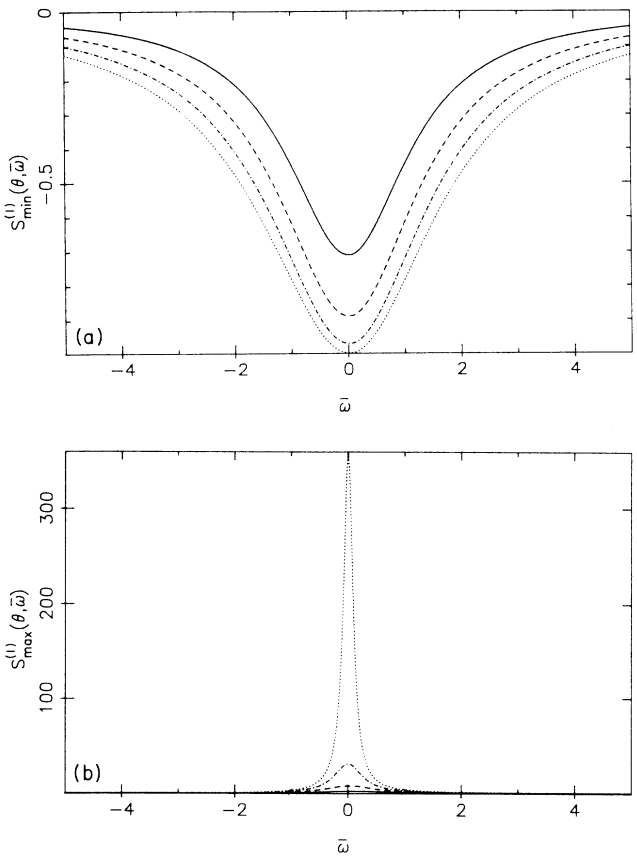

FIG. 3. Squeezing $S^{(1)}(\theta,\omega)$ vs frequency, on resonance, for a range of input powers and equal relaxation times: $P=0.3,0.5,0.7,0.9$. Plotted are minimal fluctuations $S^{(1)}(\pi/2,\omega)$ in (a) ($P=0.9$ gives *lowest* fluctuations); maximal fluctuations $S^{(1)}(0,\omega)$ in (b) ($P=0.9$ gives greatest fluctuations in this case). Here, $\eta=1$.

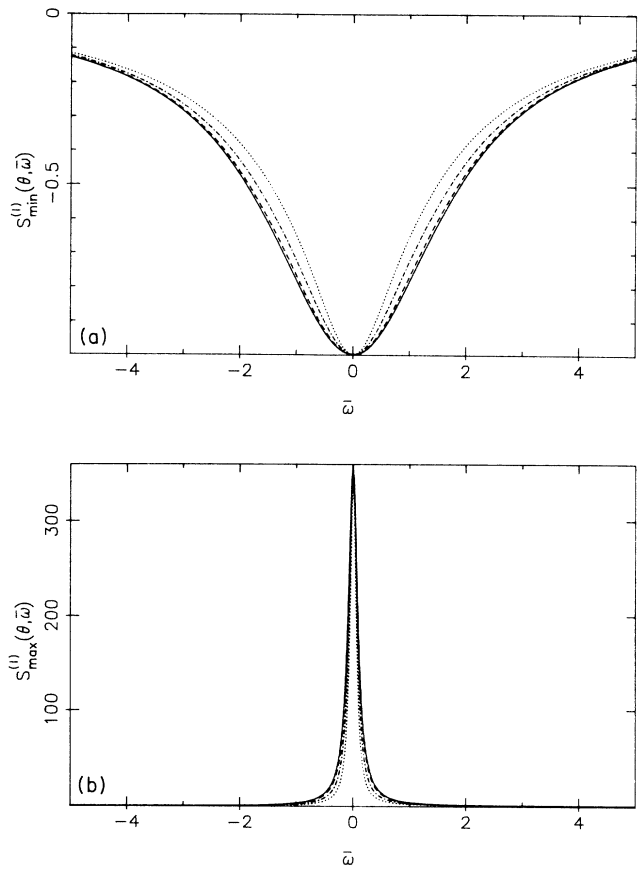

FIG. 4. Squeezing $S^{(1)}(\theta,\omega)$ vs frequency, on resonance, for varoius ratios of decay rates in the absence of detunings. Plotted are $\kappa_2^0/\kappa_1^0=1,2,4,8$. (a) gives the minimum fluctuations and (b) gives the largest fluctuations, as the phase angle is varied. Here $P=0.9$, $\eta=1$.

broadband field.

The next case we consider is that of equal cavity decay rates ($\kappa_1^0=\kappa_2^0=\kappa^0$), but with nonzero detuning $\bar{\Delta},\Delta_3$. Even for $\Delta_3=0$, we allow for a nonzero $\bar{\Delta}$. This accounts for dispersion effects which could mean the matching condition $\omega_1+\omega_2\sim\omega_3$ is only approximate. Where $\omega_1+\omega_2=\omega_3$, we have $\bar{\Delta}=\Delta_3/2$. We note from the solution (5.9) that Δ_3 enters explicitly only in α_3^0 and hence simply rotates the optimal phase angle θ. The eigenvalue solutions in this case are

$$\lambda_{1/2}=\lambda_{3/4}^{*}=-\kappa^0\pm\tfrac{1}{2}(x_+ +ix_-)\ . \tag{6.5}$$

Here x_+ and x_- are defined for $P^2(1+\bar{\Delta}^2)<\bar{\Delta}^2$, as

$$\begin{aligned} x_+ &=0\ , \\ x_- &=2\kappa^0[\bar{\Delta}^2-P^2(1+\bar{\Delta}^2)^{1/2}]\ , \end{aligned} \tag{6.6}$$

while if $P^2(1+\bar{\Delta}^2)>\bar{\Delta}^2$, they are defined as

$$\begin{aligned} x_+ &=2\kappa^0[P^2(1+\bar{\Delta}^2)-\bar{\Delta}^2]^{1/2}\ , \\ x_- &=0\ . \end{aligned} \tag{6.7}$$

For low driving fields E, the eigenvalues are complex and the spectrum comprises two Lorentzian side peaks. As the driving field increases, the side peaks move closer together, finally coalescing. For driving fields E such that $|E|/E_T>\bar{\Delta}^2/(1+\bar{\Delta}^2)$, the spectral components are both centered at $\omega=0$, but are characterized by different widths. As threshold is approached, one component narrows and diverges, while the other component remains broadband. Figures 5 and 6 plot the optimal squeezing spectrum for the case of symmetric decay rates and for a range of detunings. The spectrum becomes double peaked for sufficiently large detunings, even at higher pump intensities. This corresponds to resonance with the true cavity mode frequency. We note that significant noise reduction is possible at these side peaks, particularly at higher pump intensities. The effective of the detunings is to increase the bandwidth over which significant squeezing is available. Also, however, the actual pump power needed to obtain a certain amount of squeezing is increased (since E_T increases).

Figures 7 and 8 plot squeezing spectra for the situation of asymmetrical decay rates ($\kappa_1^0\pm\kappa_2^0$) with nonzero detunings. A clear asymmetry in the spectra is apparent. Plotted in the figures is $S^{(1)}(\theta,\omega)$, which is the half of the squeezing spectrum [Eq. (6.1)] centered at the frequency $\omega_0+\epsilon$ (the other half of the spectrum centered at $\omega_0-\epsilon$ is

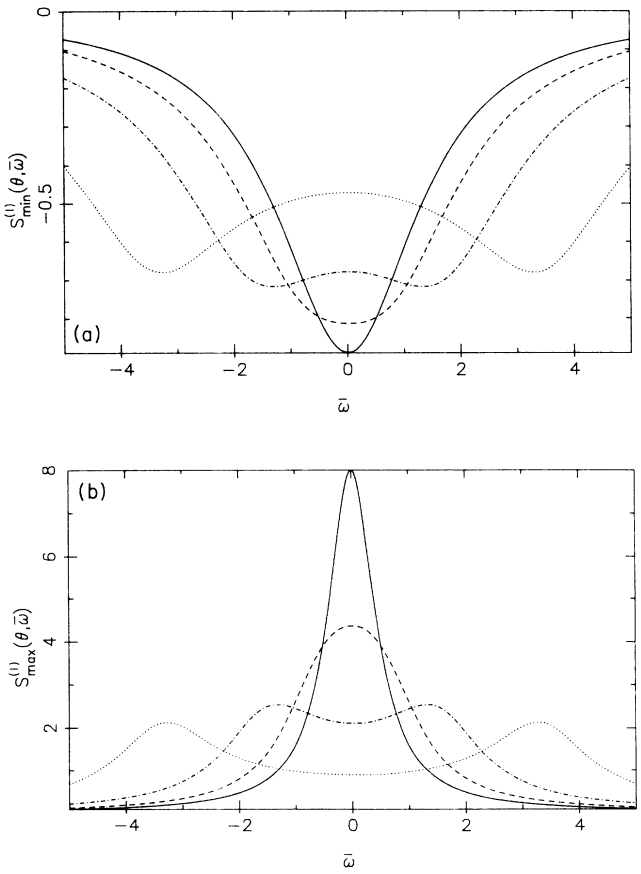

FIG. 5. Squeezing vs frequency off resonance, for a range of input detunings and equal relaxation times. Here $\bar{\Delta}=0,1,3,4$; $P=0.5$. Plotted are minimal fluctuations in (a); maximal fluctuations in (b). In each case, $\bar{\Delta}=0$ is the narrowest and $\bar{\Delta}=4$ is the broadest graph. Here, $\eta=1$.

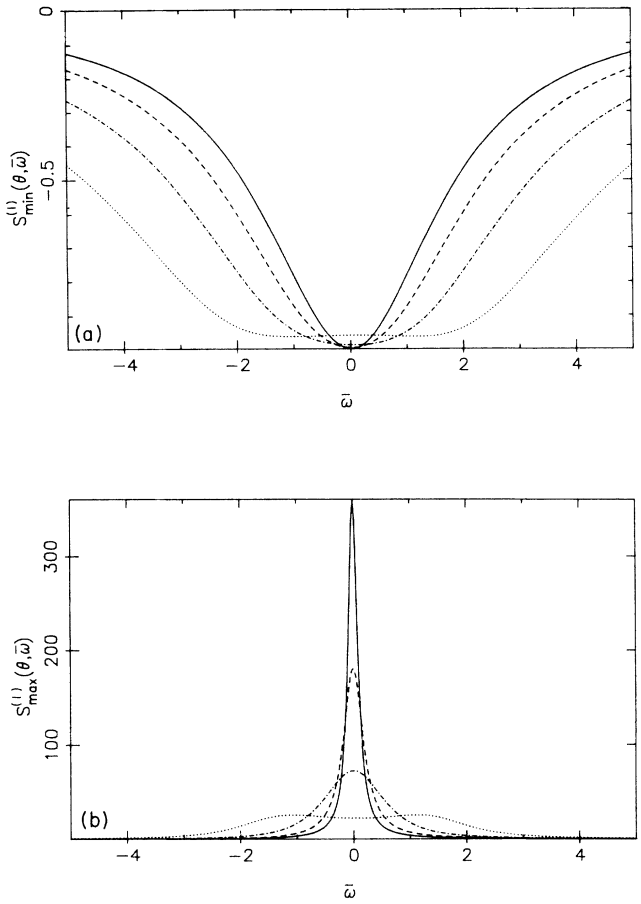

FIG. 6. As in Fig. 5, but with $P=0.9$, nearer the critical point.

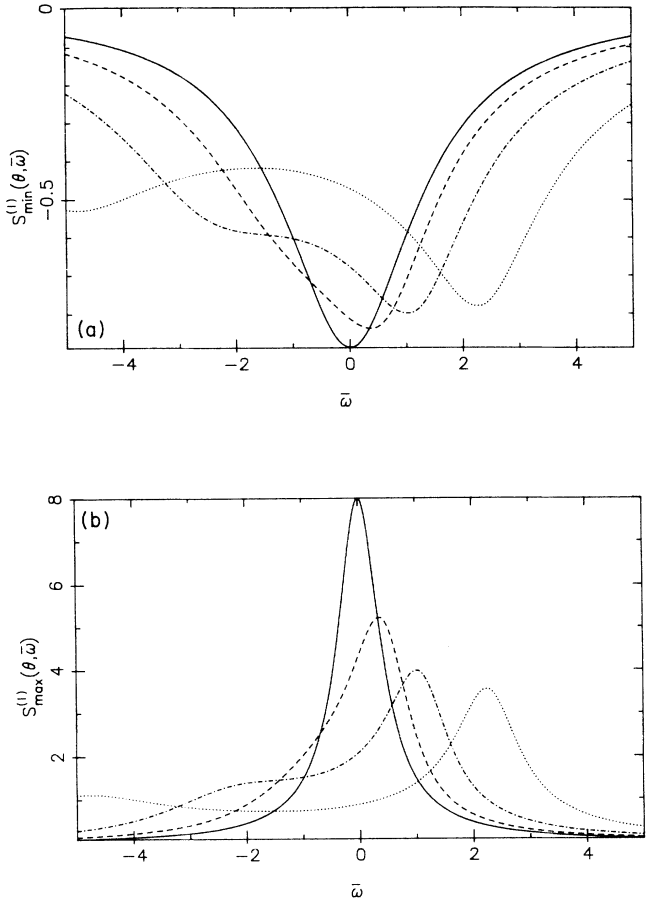

FIG. 7. Squeezing $S^{(1)}(\theta,\omega)$ vs frequency off resonance, for a range of detunings and unequal relaxation times. Here $\bar{\Delta}=0,1,2,4$; $\kappa_2^0/\kappa_1^0=2$, $P=0.5$. Plotted are minimal fluctuations in (a); maximal fluctuations in (b). In each case, $\bar{\Delta}=0$ is the narrowest and $\bar{\Delta}=4$ is the broadest graph. Here, $\eta=1$.

the mirror image). The increasing ω corresponds to frequencies greater than $\omega_0+\epsilon$. Thus we note a reduction of squeezing for quadrature components whose frequencies are nearest the frequency of the cavity mode which is more heavily damped. There is a corresponding increase in squeezing for the frequencies closer to the other cavity mode frequency.

VII. SQUEEZING WITH TWIN LOCAL OSCILLATORS

We now focus attention on the dual-local-oscillator and detector measurements discussed in Sec. III. Measurements of this type have been performed by Levenson *et al.* and Schumaker *et al.*,[25] and similar intensity-correlation measurements by Heidmann *et al.*[17] The use of two local oscillators means one can detect individually a particular quadrature phase amplitude of each of the signal and idler fields. The quadrature amplitudes for each field are defined, in the case of perfect detectors, as

$$\hat{X}_i^{\theta_i}(t)=\hat{\Phi}_i(t)e^{i(\theta_i+\omega_i^0 t)}+[\Phi_i(t)]^\dagger e^{-i(\theta_i+\omega_i^0 t)} . \quad (7.1)$$

Here $i=1$ denotes the signal field associated with mode $\hat{a}_1$, and $i=2$ denotes the idler field associated with mode $\hat{a}_2$. The photocurrents $i_i(t)$ contain information about the detected quadrature phase amplitude. The individual photocurrents may be amplified by a factor of Z_i as defined in Sec. III, and then combined to yield a total current of

$$i_T(t)\sim i_1(t)\pm i_2(t) . \quad (7.2)$$

This total current contains information about the corresponding combined quadrature phase amplitude operators. The squeezing in a combined amplitude of this type has been studied recently by Schumaker *et al.*[25,35] and has been called "four-mode squeezing."

The total current is also useful in treating the case of a single detector with orthogonally polarized beams. In this case, the two independent polarizations of the local oscillator, with intensities I_1^0 and I_2^0, are regarded as the two local oscillators. The output current of the detector is then the sum of the two terms arising from the photo-

detector response to the two orthogonal polarizations. This is physically different from the earlier cases, as the two input beams have no coherent interference term, which would occur if they had parallel polarizations.

It is shown in Sec. III that the normalized power spectrum of such a combined current is given by $V_{\pm}(\theta_1,\theta_2,\omega)$. This spectrum may be reexpressed for perfect efficiency ($\eta=1$), in terms of non-normally ordered moments. Thus, in the case of the difference current spectrum,

$$V_{\pm}(\theta_1,\theta_2,\omega)=\frac{1}{1+g^2}\int_{-\infty}^{\infty}e^{-i\omega t}\langle[\hat{X}_1^{\theta_1}(0)\pm g\hat{X}_2^{\theta_2}(0)][\hat{X}_1^{\theta_1}(\tau)\pm g\hat{X}_2^{\theta_2}(\tau)]\rangle d\tau\ , \tag{7.3}$$

and the solution is, from Eq. (3.34) with $\eta=1$,

$$V_{\pm}(\theta_1,\theta_2,\omega)=1+\frac{2}{1+g^2}[s_{11}(\omega)+g^2 s_{22}(\omega)]\pm\frac{2g}{1+g^2}\mathrm{Re}\{e^{i(\theta_1+\theta_2)}[c_{12}(\omega)+c_{21}(\omega)]\}\ . \tag{7.4}$$

If we consider the case of zero detunings and equal decay rates $\kappa_1^0=\kappa_2^0$, this result for the difference current simplifies to

$$V_{\pm}(\theta_1,\theta_2,\omega)=1+2s_{11}(\omega)\pm\frac{4g}{1+g^2}\cos(\theta_1+\theta_2)c_{12}(\omega)\ , \tag{7.5}$$

since $s_{11}(\omega)=s_{22}(\omega)$ and $c_{12}(\omega)=c_{21}(\omega)$. Choosing $\theta_1+\theta_2=\pi$ for V_+, and $\theta_1+\theta_2=0$ for V_-, with equal gain ($g=1$), we obtain

$$V_+(\theta_1,\pi-\theta_1,\omega)=V_-(\theta_1,-\theta_1,\omega)=1-\frac{4P}{(P+1)^2+\bar{\omega}^2}\ . \tag{7.6}$$

A perfect suppression of the shot-noise level is predicted near threshold and at zero frequency. The second term in this function is plotted in Fig. 3. The reduction in noise indicates a correlation between the particular quadrature operators $\hat{X}_1^{\theta_1}$ and $\hat{X}_2^{\theta_2}$ in frequency space. This indicates the presence of "four-mode squeezing," which is a nonclassical property of the radiation field.

To facilitate a discussion in frequency space, we consider the normalized Fourier-transformed quadrature operator

$$\hat{x}_j^{\theta_j}(\omega)=\frac{1}{\sqrt{T}}\int_{-T/2}^{T/2}e^{i\omega\tau}\hat{X}_j^{\theta_j}(t)dt\ . \tag{7.7}$$

Here we introduce the observation time T for normalization of the quadrature operator commutation relations. We intend to take T large but finite (i.e., $T\gg\kappa^{-1}$), so Fourier-transform identities are approximately valid. In cases of perfect efficiency, the power spectrum in terms of these components may be written, using the fact that $[x_j^{\theta_j}(\omega)]^{\dagger}=x_j^{\theta_j}(-\omega)$ and the result Eq. (3.34), as

$$V_{\pm}(\theta_1,\theta_2,\omega)=\frac{1}{1+g^2}\langle[\hat{x}_1^{\theta_1}(-\omega)\pm g\hat{x}_2^{\theta_2}(-\omega)]\times[\hat{x}_1^{\theta_1}(\omega)\pm g\hat{x}_2^{\theta_2}(\omega)]\rangle\ . \tag{7.8}$$

It should be noted that the Fourier quadrature operator $\hat{x}_j^{\theta_j}(\omega)$ itself is not a Hermitian operator. As discussed by Schumaker[23] and Leverson and Shelby,[25] one may, however, define real and imaginary parts which are Hermitian. It is these real and imaginary parts, or a linear combination of these operators, which are the measurable quadrature observables at the detectors. Let us write

$$\hat{x}_j^{\theta_j}(\omega)=\mathrm{Re}[\hat{x}_j^{\theta_j}(\omega)]+i\ \mathrm{Im}[\hat{x}_j^{\theta_j}(\omega)]\ , \tag{7.9}$$

and

$$\hat{x}_-(\omega)=\hat{x}_1^{\theta_1}(\omega)-g\hat{x}_2^{\theta_2}(\omega)=\mathrm{Re}[\hat{x}_-(\omega)]+i\ \mathrm{Im}[\hat{x}_-(\omega)]\ .$$

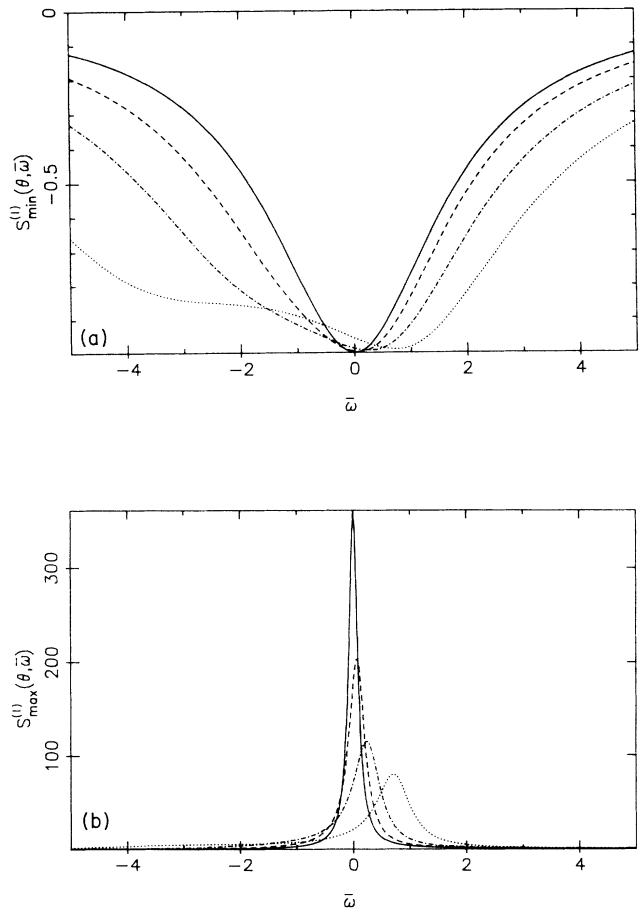

FIG. 8. As in Fig. 7, but with $P=0.9$, near the critical point.

The correlation between, say, $\mathrm{Re}[\hat{x}_1^{\theta_1}(\omega)]$ and $\mathrm{Re}[\hat{x}_2^{\theta_2}(\omega)]$, is obtained by measuring the noise quantity of Eq. (7.8). The associated (stationary) power spectrum may be denoted

$$\langle |x_-(\omega)|^2 \rangle \equiv \langle [\hat{x}_-(\omega)]^\dagger \hat{x}_-(\omega) \rangle = \langle \{\mathrm{Re}[\hat{x}_-(\omega)]\}^2 \rangle + \langle \{\mathrm{Im}[\hat{x}_-(\omega)]\}^2 \rangle \tag{7.10}$$

For the particular type of field we consider, the correlation properties of $\mathrm{Re}[\hat{x}_j^{\theta_j}(\omega)]$ and $\mathrm{Im}[\hat{x}_j^{\theta_j}(\omega)]$ are identical, and the $\mathrm{Re}[\hat{x}_j^{\theta_j}(\omega)]$ and $\mathrm{Im}[\hat{x}_j^{\theta_j}(\omega)]$ are uncorrelated. Hence $\langle |\hat{x}_-(\omega)|^2 \rangle$ is the measure of the total variance of the difference between signal and idler quadrature observables, regardless of which particular linear combination of real and imaginary parts we would choose as our signal. Thus where the noise level $V_-(\theta_1,\theta_2,\omega) \to 0$, there is a perfect correlation between both the real and imaginary parts of the quadrature operators $\hat{x}_1^{\theta_1}(\omega), \hat{x}_2^{\theta_2}(\omega)$.

These results demonstrate the existence of four-mode squeezing in the current-difference observable. We note that this can be distinguished from having two independently squeezing quadrature fields at the two detectors. In the case of the nondegenerate parametric oscillator, the four-mode squeezing depends on the sum of the quadrature phase angles, not on the angles individually. An alternative way to demonstrate that the quadratures have nonclassical correlations is through the Cauchy-Schwarz inequality derived in Sec. III:

$$\langle \hat{x}_1^{\theta_1}(-\omega)\hat{x}_1^{\theta_1}(\omega) \rangle \langle \hat{x}_2^{\theta_2}(-\omega)\hat{x}_2^{\theta_2}(\omega) \rangle \geq |\langle \hat{x}_1^{\theta_1}(-\omega)\hat{x}_2^{\theta_2}(\omega) \rangle|^2 . \tag{7.11}$$

The inequality implies maximum correlation between $\hat{x}_1^{\theta_1}(\omega)$ and $\hat{x}_2^{\theta_2}(\omega)$ when the correlation coefficient

$$\frac{|\langle \hat{x}_1^{\theta_1}(-\omega)\hat{x}_2^{\theta_2}(\omega) \rangle|^2}{\langle |\hat{x}_1^{\theta_1}(\omega)|^2 \rangle \langle |\hat{x}_2^{\theta_2}(\omega)|^2 \rangle} \tag{7.12}$$

becomes equal to 1.

We see from the derivation in Sec. III of the Cauchy-Schwarz inequality that if the equality (7.11)] is satisfied, then there exists a choice of g [given by Eq. (3.41)] such that the variance $V_-(\theta_1,\theta_2,\omega)$ is zero. The measurement of $V_-(\theta_1,\theta_2,\omega)$ is a suitable way to obtain information about correlation. In fact, it may be used to infer sufficient correlation to violate the classical Cauchy-Schwarz inequality [Eq. (3.44)]. We can write

$$V_\pm(\theta_1,\theta_2,\omega) = 1 + S_\pm(\theta_1,\theta_2,\omega)/(1+g^2) ,$$

where

$$S_\pm(\theta_1,\theta_2,\omega) = \langle :|\hat{x}_1^{\theta_1}(\omega) \pm g\hat{x}_2^{\theta_2}(\omega)|^2: \rangle . \tag{7.13}$$

With the relative gain (g) chosen so that $g = g_c$ for the case of V_- and $g = -g_c$ for the case of V_+, where

$$g_c = \frac{\langle \hat{x}_2^{\theta_2}(-\omega)\hat{x}_1^{\theta_1}(\omega) \rangle}{\langle :\hat{x}_2^{\theta_2}(-\omega)\hat{x}_2^{\theta_2}(\omega): \rangle} , \tag{7.14}$$

we find that $S_\pm$ reduces to an optimal combined squeezing $S^{(c)}$, where

$$S_\pm^{(c)}(\theta_1,\theta_2,\omega) = \langle :\hat{x}_1^{\theta_1}(-\omega)\hat{x}_1^{\theta_1}(\omega): \rangle - \frac{|\langle \hat{x}_2^{\theta_2}(-\omega)\hat{x}_1^{\theta_1}(\omega) \rangle|^2}{\langle :\hat{x}_2^{\theta_2}(-\omega)\hat{x}_2^{\theta_2}(\omega): \rangle} . \tag{7.15}$$

A violation of the classical Cauchy-Schwarz inequality (3.44) thus implies $S_\pm^{(c)} < 0$. Thus a violation of the Cauchy-Schwarz inequality implies that there exists a choice of g (namely g_c) which will allow a squeezing of the combined field: $V_-(\theta_1,\theta_2,\omega) < 1$. In fact, the reverse statement is also true. It is possible to show that the choice g_c corresponds to the minimum value of S_-. Hence, if squeezing is observed in the combined field so that $V_-(\theta_1,\theta_2,\omega) < 1$, this implies $S_- < 0$, and hence that $S_\pm^{(c)} < 0$. This is a violation of the classical Cauchy-Schwarz inequality. We mention this because it is often easier in some experimental situations to measure the difference power spectrum as opposed to the correlation products directly. Thus we point out the equivalence of "squeezing" to this violation of the classical Cauchy-Schwarz inequality. In fact, a squeezing of a variance of the type $V_-(\theta_1,\theta_2,\omega)$, and hence, an implicit violation of the classical Cauchy-Schwarz inequality, has already been observed by Schumaker *et al.*[25] and by Heidmann *et al.*[17]

For the system studied here, the results of Eqs. (3.30) and of (5.11) and (5.12) can be utilized directly in the resonant symmetrical decay case, with $g = 1$, to show that

$$\langle x_1^{\theta_1}(-\omega)x_2^{\theta_2}(\omega) \rangle = 2P\cos(\theta_1+\theta_2) \times \left[\frac{1}{(1-P)^2+\bar{\omega}^2} + \frac{1}{(1+P)^2+\bar{\omega}^2} \right] , \tag{7.16}$$

and

$$\langle \hat{x}_i^{\theta_i}(-\omega)x_i^{\theta_i}(\omega): \rangle = 2P \left[\frac{1}{(1-P)^2+\bar{\omega}^2} - \frac{1}{(1+P)^2+\bar{\omega}^2} \right] . \tag{7.17}$$

For $\cos(\theta_1+\theta_2) = 1$ (i.e., $\theta_1+\theta_2 = 0$), the classical Cauchy-Schwarz inequality is violated, indicating the existence of greater than classical correlations between the signal and idler quadrature phases. As pointed out in Sec. III, a correlation strong enough to produce a noise level below the shot-noise level [$V_-(\theta_1,\theta_2,\omega) < 1$] cannot be ascribed to fields represented in the positive Glauber-Sudarshan P representation. The dual-detector experiments thus provide a means of testing for quantum correlation in the quadrature phase between signal and idler.

Dual-beam intensity correlations and systems which violate a classical Cauchy-Schwarz inequality in intensity correlations have been discussed previously.[14,36]

VIII. NONLOCAL INFERENCE OF QUADRATURE AMPLITUDES

The dual-local-oscillator experiments give direct information about correlation between two quadrature phases. The correlation between particular quadrature phase amplitudes of the signal and idler fields allows one to perform nondestructive measurements of the signal. One may make a homodyne measurement of the idler amplitude $\hat{x}_2^{\theta}(\omega)$, for example, and hence infer from it the value of the signal amplitude $\hat{x}_1^{-\theta}(\omega)$. The nondegenerate parametric oscillator and systems closely related to it have recently[25,26] been considered in potential quantum nondemolition measurement[37] schemes. The correlation between signal and idler intensities in the parametric oscillator above threshold also has potential application in absorption spectroscopy.[17]

In a realistic situation, the correlation between quadrature phase operators $x_1^{\theta_1}(\omega)$ and $x_2^{\theta_2}(\omega)$ will not be maximum. The result [Eq. (7.6)] for the ideal parametric oscillator indicates a small, but still nonzero, noise level $[V_-(\theta,-\theta,\omega)>0]$ over accessible frequencies. The important question then is to what precision can we infer the signal quadrature amplitude $\hat{x}_1^{\theta_1}(\omega)$, given a measurement of the idler amplitude $\hat{x}_2^{\theta_2}(\omega)$. Let us suppose we measure $\hat{x}_2^{\theta_2}(\omega)$ and obtain a result $x_2(\omega)$. We write our estimate of $\hat{x}_1^{\theta_1}(\omega)$, given this result, as $x_1(\omega)$, where

$$x_1(\omega)=g x_2(\omega) . \tag{8.1}$$

Later we shall define g to be $\tilde{g}$, where $\tilde{g}$ is a number determined in such a way as to give the best estimate for $\hat{x}_1^{\theta_1}(\omega)$. The error in this estimate for an arbitrary value of g is given by

$$[\Delta^2(\theta_1,\theta_2,g,\omega)]_R=\langle|\hat{x}_1^{\theta_1}(\omega)-x_1(\omega)|^2\rangle_R . \tag{8.2}$$

Here, R indicates the conditional average given the result $x_2(\omega)$ for the $\hat{x}_2^{\theta_2}$ measurement. Averaging over all outcomes of the $\hat{x}_2^{\theta_2}$ measurement, we therefore define an overall variance of

$$\Delta^2(\theta_1,\theta_2,g,\omega)=\langle|\hat{x}_1^{\theta_1}(\omega)-g\hat{x}_2^{\theta_2}(\omega)|^2\rangle . \tag{8.3}$$

We note that this corresponds to the difference operator $\hat{x}_-(\omega)$, where

$$\hat{x}_-(\omega)=\hat{x}_1^{\theta_1}(\omega)-g\hat{x}_2^{\theta_2}(\omega) . \tag{8.4}$$

If the output fields are in an eigenstate of $\hat{x}_-(\omega)$, then the variance of $\hat{x}_-(\omega)$ is zero. In this case the "state of the signal field upon idler readout" is an eigenstate of $\hat{x}_1^{\theta_1}(\omega)$ with the value $x_1(\omega)$, i.e., the result of subsequent immediate measurement of the signal $\hat{x}_1^{\theta_1}$ gives, with certainty, the result $x_1(\omega)$. Of course, where the quantum system is not an eigenstate of $\hat{x}_-(\omega)$, this is not the case, and there is a distribution of values, say, $\hat{x}_R^{\theta_1}(\omega)$, obtained over a series of such measurements made on an ensemble of identically prepared systems.

Clearly, because of the correlation existing between $\hat{x}_1^{\theta_1}(\omega)$ and $\hat{x}_2^{\theta_2}(\omega)$, we expect the variance in $\hat{x}_R^{\theta_1}(\omega)$ to be much smaller than the variance of $\hat{x}_1^{\theta_1}(\omega)$. The factor g is now chosen to produce the best estimate of $\hat{x}_1^{\theta_1}(\omega)$, in the sense of minimizing the variance $\Delta^2(\theta_1,\theta_2,g,\omega)$. Simple differentiation gives a value of $g=\tilde{g}$, where

$$\tilde{g}=\frac{\langle\hat{x}_2^{\theta_2}(-\omega)\hat{x}_1^{\theta_1}(\omega)\rangle}{\langle\hat{x}_2^{\theta_2}(-\omega)\hat{x}_2^{\theta_2}(\omega)\rangle} . \tag{8.5}$$

The corresponding minimum variance is, writing out the quadrature phase angles in full,

$$\begin{aligned}\Delta^2(\theta_1,\theta_2,\tilde{g},\omega)&=\langle\hat{x}_1^{\theta_1}(-\omega)\hat{x}_1^{\theta_1}(\omega)\rangle\\&\quad-\frac{|\langle\hat{x}_2^{\theta_2}(-\omega)\hat{x}_1^{\theta_1}(\omega)\rangle|^2}{\langle\hat{x}_2^{\theta_2}(-\omega)\hat{x}_2^{\theta_2}(\omega)\rangle}\\&=V_{11}(\theta_1,\theta_1,\omega)\\&\quad-|V_{21}(\theta_2,\theta_1,\omega)|^2/V_{22}(\theta_2,\theta_2,\omega) .\end{aligned} \tag{8.6}$$

Note that $g=\tilde{g}$ is defined by the minimization procedure, and we have used Eq. (3.28) for the case of perfect detector efficiency to express the result in terms of observed variances.

We now specialize to our particular system and solutions. We consider the case of equal decay rates $\kappa_2^0=\kappa_1^0$ and no detunings. This implies that $\tilde{g}$ and $c_{21}(\omega)$ are real. In terms of the definitions $s_{ij}(\omega)$ and $c_{ij}(\omega)$, we would have written

$$\begin{aligned}\Delta^2(\theta_1,\theta_2,g,\omega)&=1+\tilde{g}^2+s_{11}(\omega)+s_{11}(-\omega)\\&\quad+\tilde{g}^2[s_{22}(\omega)+s_{22}(-\omega)]\\&\quad-2\tilde{g}\,\mathrm{Re}\{[c_{12}(\omega)+c_{21}(\omega)]e^{i(\theta_1+\theta_2)}\} .\end{aligned} \tag{8.7}$$

In this system the variance is minimized with the choice $\tilde{\theta}_2=-\theta_1$.

The optimal value of g is then

$$\tilde{g}=\frac{c_{12}(\omega)+c_{21}(\omega)}{1+s_{22}(\omega)+s_{22}(-\omega)} . \tag{8.8}$$

The corresponding minimal value of $\Delta^2(\theta_1,\theta_2,\tilde{g},\omega)$ at the optimal phase angle $\tilde{\theta}_2$ is denoted $\Delta^2(\theta_1,\omega)$, where

$$\begin{aligned}\Delta^2(\theta_1,\omega)&=1+s_{11}(\omega)+s_{11}(-\omega)\\&\quad-\frac{c_{12}(\omega)+c_{12}(\omega)}{1+s_{22}(\omega)+s_{22}(-\omega)} .\end{aligned} \tag{8.9}$$

We see immediately that where one has perfect squeezing, the variance $\Delta^2(\theta_1,\omega)$ is zero. This corresponds to a maximum correlation between $\hat{x}_1^{\theta_1}(\omega)$ and $\hat{x}_2^{-\theta_1}(\omega)$.

In general, however, the squeezing variance $V_-(\theta_1,\theta_2,\omega)$ and the "inference" variance $\Delta^2(\theta_1,\theta_2,g,\omega)$ are quite different and have different physical interpretations. Squeezing occurs when $V_-(\theta_1,\theta_2,\omega)<1$ or

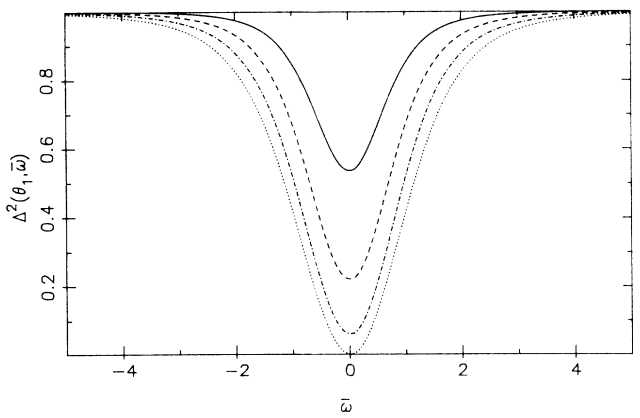

FIG. 9. The inference spectrum $\Delta^2(\theta_1,\omega)$ on resonance for a range of input powers and with equal relaxation times: $P=0.3,0.5,0.7,0.9$; $\eta=1$.

$\Delta^2(\theta_1,\theta_2,g,\omega)<1+|g|^2$. Squeezing is not necessarily minimized by the choice of $g=\bar{g}$ and refers to a total noise reduction relative to the combined shot-noise level on both signal and idler detectors. The $\Delta^2(\theta_1,\theta_2,g,\omega)$, however, is minimized relative to the shot-noise level of the signal alone and is relevant in, for example, establishing quantum nondemolition (QND) measurements.[25] In fact, such an inference variance has been discussed and measured by Levenson and Shelby[25] in broadband four-wave mixing using optical fibers. Because in general $\bar{g}$ is dependent on, for example, frequency ω, the $\Delta^2(\theta_1,\omega)$ spectrum and squeezing spectrum look quite different. The $\Delta^2(\theta_1,\omega)$ spectrum is plotted in Fig. 9.

We point out that such correlations between the quadrature phase amplitudes provide an example of the EPR paradox. This is discussed in previous publications[29,30] on parametric amplifier experiments. The EPR paradox was an argument put forward by Einstein, Podolsky, and Rosen[28] (EPR), in support of the hypothesis that a quantum-mechanical description of a physical system is incomplete. We briefly review their original argument. They considered two spatially separated particles which have, according to quantum mechanics, a maximum correlation of their positions, as well as a correlation of their momenta. Thus a measurement of the position of particle 2 implies with certainty a particular result if the position of particle 1 is measured immediately. Assuming there is no action-at-a-distance, the prediction for the position of particle 1 is made without disturbing the particle. Hence EPR identify with particle 1 a predetermined definite value of its position. The momenta of the two particles is also correlated and hence by similar arguments EPR were led to ascribe to particle 1 a definite predetermined value of its momentum. This seems to imply tha particle 1 can be thought of as having a definite value of both position and momentum. In quantum mechanics such a description is contrary to the uncertainty principle. EPR deduced from this argument that the quantum-mechanical description is in some sense incomplete. A subsequent version of the paradox involving correlations between spin components of two spatially separated particles was presented by Bohm. The Bohm correlations, however, involve completely different operators from the EPR proposal. Experimental demonstrations of the Bell inequalities are associated with this latter version, although there have been recent suggestions relating to the original version.[38]

The original EPR paradox can be formulated in terms of the correlated quadrature phase amplitudes of the nondegenerate parametric amplifier. We examine the solution of Eq. (8.7) for the variance and note the angular dependence, $\theta_1+\theta_2=0$, required for minimum variance. According to Eq. (8.9) as plotted in Fig. 9, as we approach threshold the zero-frequency components $\hat{x}^{\theta_1}(0)$ and $\hat{x}^{-\theta_1}(0)$ are (in principle) perfectly correlated. Thus one can infer the result for $\hat{x}^{\theta_1}(0)$ by a measurement of $\hat{x}^{0}_{2}(0)$; or we could infer $\hat{x}^{\pi/2}_{1}(0)$ by a measurement of $\hat{x}^{-\pi/2}_{2}(0)$. Now $\hat{x}^{0}_{1}(0)$ and $\hat{x}^{\pi/2}_{1}(0)$ are operators whose commutators correspond precisely to position and momentum operators. The Heisenberg uncertainty relation specifies a nonzero minimum uncertainty product for their variances. Hence the correlation between $\{\hat{x}^{0}_{1},\hat{x}^{0}_{2}\}$ and $\{\hat{x}^{\pi/2}_{1},x^{-\pi/2}_{2}\}$ is an example of the EPR paradox, although in order to have causally separated observations, the two detectors would need to be separated by at least 2 cT from each other. This is a system which appears capable of experimental realization.

In a realistic experimental situation the correlation between the $x^{\theta}_{1}(\omega)$ and $\hat{x}^{-\theta}_{2}(\omega)$ will not be perfect because of losses and detector inefficiencies. Hence we will not observe $\Delta^2(\theta_1,\omega)=0$ but some finite value of the quantity $\Delta^2(\theta_1,\omega)$. We ask ourselves at what correlation has the paradox been demonstrated. This has been discussed in another paper[30] and we adopt that approach. If we measure $\hat{x}^{0}_{2}(\omega)$, then as discussed above we can infer $\hat{x}^{0}_{1}(\omega)$ with a certain precision given by the inference variance. This would lead us, assuming the EPR concept of reality and no action-at-a-distance, to assign to the signal field a predetermined range of values of $\hat{x}^{0}_{1}$ with an associated variance $\Delta^2(0,\omega)$. Similarly, we could measure $\hat{x}^{-\pi/2}_{2}(\omega)$, and infer from this an average value for $\hat{x}^{\pi/2}_{1}(\omega)$ with associated variance $\Delta^2(\pi/2,\omega)$. Thus we also associate with the signal field a predetermined range of values of $\hat{x}^{\pi/2}_{1}$ with a certain variance. Now if our inferred variances are such that

$$\Delta^2(0,\omega)\Delta^2(\pi/2,\omega)<1\ , \tag{8.10}$$

we have the EPR contradiction between quantum mechanics and local realism.

In order to verify that the inequality of Eq. (8.10) holds, experimental variance measurements are required at the two complementary phase angles of 0 and $\pi/2$. We note that since the local-oscillator phase angles can be adjusted at each detector independent, it is possible to have delayed choice of the type of measurement used. This removes to some extent the famous objection of Bohr to the EPR paradox, namely that local realism must involve a specification of the measurement technique.

In the case of a measurement that directly produces the correlation of the output currents, Eq. (8.9) can be expressed as the following inequality between the observed variances and correlations (for perfect detector efficiency):

$$[V_{22}(0,0,0)V_{11}(0,0,0)-|V_{21}(0,0,0)|^2][V_{22}(\pi/2,\pi/2,0)V_{22}(-\pi/2,-\pi/2,0)-|V_{21}(\pi/2,-\pi/2,0)|^2] \leq V_{22}(0,0,0)V_{22}(\pi/2,\pi/2,0) . \quad (8.11)$$

The above expression can be generalized to the case of finite-frequency correlation measurements, although as remarked earlier, the usual finite-frequency measurements, in fact, involve a pair of Hermitian operators at each frequency point. For this reason, an additional assumption that there is no cross correlation between the real and imaginary parts is required. While this is true in our theoretical treatment, it does not appear to be necessarily true in general.

In practice, it is often simpler to measure the $V_{\pm}$ variances than the V_{ij} variances. Since these variances are normalized by the total shot noise, the equation corresponding to (8.10) at any given gain g is just

$$V_{-}(0,0,\omega)V_{-}(\pi/2,-\pi/2,\omega) < \frac{1}{(1+g^2)^2} . \quad (8.12)$$

This is generally harder to obtain than just squeezing, owing to the $1/(1+g^2)^2$ factor. Thus a direct subtraction of currents with $g=1$ would require at least 50% squeezing before an inferred violation of the Heisenberg uncertainty principle is obtained.[29] This, however, is not the optimal choice of g. It is possible to calculate from a complete set of measurements at any g value, whether the optimal choice of g would give correlations that are strong enough to satisfy Eq. (8.10).

A similar version of the paradox has been discussed by Paul,[39] who considers the phase and intensity correlations of two spatially separated beams. With the recent success[7] in degenerate parametric oscillation in measuring noise reduction below the coherent state level in one of the quadrature phase amplitudes, our proposal for the nondegenerate parametric oscillator would seem feasible. We note that the operators we choose here correspond precisely in their algebraic properties to those utilized in the EPR paper. The experimental verification of the violation of Bell's inequalities was restricted to operators with a spin-$\frac{1}{2}$ algebra, with a completely different eigenvalue spectrum to that proposed by EPR. The nondegenerate parametric oscillator appears to be capable of reproducing the precise type of quantum-mechanical correlations required to demonstrate the original EPR paradox. Further, since quadrature detection is a highly efficient process, this experiment would not have the problems associated with inefficient photodetection in the usual photon correlation experiments that test the Bell inequalities.

IX. DISCUSSION

We have analyzed the below-threshold correlations in the signal and idler fields of a nondegenerate parametric oscillator. A detailed analysis of single- and double-local-oscillator measurements has been given, using a normally ordered photodetector theory. This allows us to directly use the results of a normally ordered stochastic theory for the quantum correlations in the output, and their spectra. The results imply that good squeezing exists including detuning and unequal decay rates.

We have also analyzed nonclassical correlations between the output quadratures. Conditions for nonclassical correlations are calculated using a Cauchy-Schwarz inequality, which is violated over a range of local-oscillator phase angles. From the point of view of the EPR paradox, an apparent violation of the Heisenberg uncertainty principle occurs, using inferred measurement to obtain the value of two complementary variables. This allows the possibility of a new test of quantum mechanics in the area proposed by Einstein, Podolsky, and Rosen. We note that this test is different from the Bell inequality tests, as it involves variables with continuous spectra, which have an identical operator algebra to that originally suggested.

[1] H. Takahashi, Adv. Commun. Syst. **1**, 227 (1965); for a review, see D. F. Walls, Nature (London) **306**, 141 (1983).

[2] D. Stoler, Phys. Rev. D **1**, 3217 (1970); **4**, 1935 (1971).

[3] H. P. Yuen, Phys. Rev. A **13**, 2226 (1979).

[4] C. M. Caves, Phys. Rev. D **26**, 1817 (1980).

[5] M. Xiao, L. Wu, and H. J. Kimble, Phys. Rev. Lett. **59**, 278 (1987).

[6] R. E. Slusher, L. W. Hollberg, B. Yurke, J. S. Mertz, and J. F. Valley, Phys. Rev. Lett. **55**, 2409 (1985); R. M. Shelby, M. D. Levenson, S. H. Perlmutter, R. S. Devoe, and D. F. Walls, *ibid.* **57**, 691 (1986); L. Wu, H. J. Kimble, J. L. Hall, and H. Wu, *ibid.* **57**, 2520 (1986); M. W. Maeda, P. Kumar, and J. M. Shapiro, Opt. Lett. **12**, 161 (1987); M. G. Raizen, L. Orozco, M. Xiao, T. L. Boyd, and H. J. Kimble, Phys. Rev. Lett. **59**, 198 (1987); S. Machida, Y. Yamamoto, and J. Itaya, *ibid.* **58**, 1000 (1987).

[7] L. Wu, M. Xiao, and H. J. Kimble, J. Opt. Soc. Am. B **4**, 1465 (1987).

[8] R. Graham, in *Quantum Statistics in Optics and Solid State Physics* (Springer, Berlin, 1973).

[9] P. D. Drummond, K. J. McNeil, and D. F. Walls, Opt. Acta **27**, 321 (1980); **28**, 211 (1981).

[10] G. J. Milburn and D. F. Walls, Opt. Commun. **39**, 401 (1981).

[11] B. Yurke, Phys. Rev. A **32**, 300 (1985).

[12] M. J. Collett and C. W. Gardiner, Phys. Rev. A **30**, 1386 (1984); M. J. Collett and D. F. Walls, *ibid.* **32**, 2887 (1985); C. M. Savage and D. F. Walls, J. Opt. Soc. Am. B **4**, 1514 (1987).

[13] R. Graham and H. Haken, Z. Phys. **210**, 276 (1968); R. Graham, *ibid.* **210**, 319 (1968); **211**, 469 (1968).

[14] K. J. McNeil and C. W. Gardiner, Phys. Rev. A **28**, 1560 (1983).

[15] M. J. Collett and R. Loudon, J. Opt. Soc. Am. B **4**, 1525

(1987).
[16]S. Reynaud, C. Fabre, and E. Giacobino, J. Opt. Soc. Am. B **4**, 1520 (1987); A. Heidmann, R. J. Horowicz, S. Reynaud, E. Giacobino, C. Fabre, and G. Camy, Phys. Rev. Lett. **59**, 2555 (1987).
[17]G. Björk and Y. Yamamoto, Phys. Rev A **37**, 125 (1988); **37**, 1991 (1988).
[18]M. D. Reid and P. D. Drummond, Phys. Rev. A **40**, 4493 (1989).
[19]R. J. Glauber, Phys. Rev. **130**, 2529 (1983); **131**, 2766 (1983).
[20]H. P. Yuen and J. H. Shapiro, IEEE Trans. Inf. Theory **IT-26**, 78 (1980); H. P. Yuen and V. W. S. Chan, Opt. Lett. **8**, 177 (1983); J. H. Shaprio, IEEE J. Quantum Electron. **QE-21**, 237 (1985); C. M. Caves and B. L. Schumaker, Phys. Rev. A **31**, 3008 (1985).
[21]Z. Y. Ou, C. K. Hong, and L. Mandel, J. Opt. Soc. Am. B **4**, 1574 (1987); H. J. Carmichael, *ibid.* **4**, 1588 (1987); M. J. Collett and R. Loudon, *ibid.* **4**, 1525 (1987).
[22]D. C. Burnham and D. L. Weinberg, Phys. Rev. Lett. **25**, 84 (1970); R. Loudon, Rep. Prog. Phys. **43**, 913 (1980); S. Friberg, C. K. Hong, and L. Mandel, Phys. Rev. Lett. **54**, 2011 (1985); E. Jakeman and J. G. Walker, Opt. Commun. **55**, 219 (1985); J. G. Walker and E. Jakeman, Opt. Acta **32**, 1303 (1985); C. K. Hong and L. Mandel, Phys. Rev. Lett. **56**, 58 (1986); R. Brown, E. Jakeman, E. Pike, J. Rarity, and P. Tapster, Europhys. Lett. **2**, 279 (1986).
[23]C. M. Caves and B. L. Schumaker, Phys. Rev. A **31**, 3068 (1985); B. L. Schumaker and C. M. Caves, *ibid.* **31**, 309 (1985).
[24]B. L. Schumaker, J. Opt. Soc. Am. A **2**, 92 (1985).
[25]B. L. Schumaker, S. H. Perlmutter, R. M. Shelby, and M. D. Levenson, Phys. Rev. Lett. **58**, 357 (1987); M. D. Levenson and R. M. Shelby, J. Mod. Opt. **34**, 755 (1987); M. D. Levenson, R. M. Shelby, M. D. Reid and D. F. Walls, Phys. Rev. Lett. **57**, 2473 (1986); H. Bachor, M. D. Levenson, D. F. Walls, S. H. Perlmutter, and R. Shelby, Phys. Rev. A **38**, 180 (1988).
[26]S. F. Pereira, H. J. Kimble, P. Alsing, and D. F. Walls (private communication).
[27]Z. Y. Ou and L. Mandel, Phys. Rev. Lett. **61**, 50 (1988).
[28]A. Einstein, B. Podolsky, and N. Rosen, Phys. Rev. **47**, 777 (1935). See also, J. F. Clauser and A. Shimony, Rep. Prog. Phys. **41**, 1881 (1978); A. Aspect, P. Grangier, and G. Roger, Phys. Rev. Lett. **47**, 460 (1981).
[29]M. D. Reid and P. D. Drummond, Phys. Rev. Lett. **60**, 2731 (1988).
[30]M. D. Reid, Phys. Rev. A **40**, 913 (1989).
[31]W. H. Louisell, *Quantum Statistical Properties of Radiation* (Wiley, New York, 1973).
[32]P. D. Drummond and C. W. Gardiner, J. Phys. A **13**, 2353 (1980); P. D. Drummond, C. W. Gardiner, and D. F. Walls, Phys. Rev. A **24**, 914 (1981)
[33]E. C. G. Sudarshan, Phys. Rev. Lett. **10**, 277 (1963).
[34]P. D. Drummond and D. F. Walls, Phys. Rev. A **23**, 2563 (1981).
[35]B. L. Schumaker, Phys. Rep. **135**, 317 (1986).
[36]M. S. Zubairy, Phys. Lett. **87A**, 162 (1982); R. Loudon, Rep. Prog. Phys. **43**, 913 (1980).
[37]C. M. Caves, K. S. Thorne, R. Drever, V. D. Sandberg, and M. Zimmermann, Rev. Mod. Phys. **52**, 341 (1980); M. Hillary and M. Scully, in *Quantum Optics Experimental Gravitational and Measurement Theory,* edited by P. Meystre and M. O. Scully (Plenum, New York, 1983); G. J. Milburn, A. Lane, and D. F. Walls, Phys. Rev. A **27**, 2804 (1983); N. Imoto, H. A. Haus, and Y. Yamamoto, *ibid.* A **32**, 2287 (1985).
[38]M. Zukowski and J. Pykacz, Phys. Lett. A **127**, 1 (1988), and references therein.
[39]H. Paul, Opt. Acta **28**, 1 (1981).